

NORTHWESTERN UNIVERSITY

Studies of Microtubule-dependent Organelle Transport in *Drosophila* S2 cells

A DISSERTATION

SUBMITTED TO THE GRADUATE SCHOOL
IN PARTIAL FULFILLMENT OF THE REQUIREMENTS

for the degree

DOCTOR OF PHILOSOPHY

Field of Cell and Molecular Biology
Integrated Graduate Program in Life Sciences

By

Hwajin Kim

CHICAGO, ILLINOIS

June 2008

ABSTRACT

Studies of Microtubule-dependent Organelle Transport in *Drosophila* S2 cells

Hwajin Kim

The proper distribution of cellular organelles and protein complexes is important for maintaining cellular organization and function. Transport in eukaryotic cells requires three motor proteins, kinesin, dynein, and myosin, attached to specific cargoes mostly by adaptor proteins. This work focuses on the mechanism of microtubule-dependent organelle transport *in vivo*.

This study examines three questions. Firstly, are motors of opposite polarity coordinated while transporting the same cargo? Intracellular organelles move along microtubules bidirectionally by kinesin and dynein, but how these motors work together is not known. This study showed that the depletion of kinesin-1 or dynein inhibited transport of peroxisomes in both directions, suggesting that peroxisomes require activities of both motors for transport.

Secondly, does dynactin, the dynein adaptor protein complex, function as a regulator between motors? Does it affect cargo transport through its microtubule binding activity? *In vitro* studies showed that dynactin increased motor processivity, but, its *in vivo* roles by microtubule binding are not known. This study used a p150^{glued} mutant (Δ N-p150^{glued}) that was truncated in the microtubule binding domain. Movement of organelles required dynactin, but Δ N- p150^{glued} did not affect the processivity, run length and velocity of transport. Dynactin binding to

microtubules is not required for cargo transport *in vivo* and although dynactin may influence transport, this effect is not mediated through microtubule binding.

Lastly, is organelle transport affected by microtubule movements? Are microtubules motile? Where do the forces that move microtubules originate? There are not many studies done on microtubule transport. This study showed that microtubules display sliding, looping, and bending movement. These microtubule movements were significantly inhibited by depletion of kinesin-1. We suggest that kinesin-1 moves (or slides) microtubules by cross-linking microtubules through its C-terminal microtubule-binding domain. We also showed that microtubule movement/sliding did not affect organelle transport.

The research presented here contributes to the understanding of microtubule-dependent transport in three ways: first, by providing evidence for interdependence between kinesin-1 and dynein; second, by exploring the role of the microtubule binding by dynactin on transport; and third, by providing a mechanism of microtubule movements mediated by kinesin-1.

ACKNOWLEDGEMENTS

I would like to thank my advisor, Vladimir Gelfand, for his guidance and support for the past four years. I am very grateful to him for accepting me as a graduate student, teaching me to think logically and critically, and guiding me on this exciting journey in research. I would also like to thank the members of the Gelfand lab, past and present, for both professional and personal relationships I formed with them. I thank Shuo-Chien Ling who as a senior member in the lab helped me both by word and example. I thank Comert Kural, Dr. Paul Selvin, Dr. Gregory Rogers, and Dr. Stephen Rogers for their collaborative efforts on the work presented in this dissertation. I would also like to thank Anna Gelfand, Minjong Park, Shabeen Ally, Lorena Bensenor, Amber Jolly, Margot Lakonishok and Shin-ichiro Kojima, for patiently listening to me and supporting me. I offer my sincere gratitude to my committee members, Dr. Jim Bartles, Dr. Adriana Ferreira, Dr. Sarah Rice and Dr. Greg Smith. I thank them for their time, attention, and valuable inputs and advice.

I would also like to thank my family and friends for their love and constant support. Most importantly, I thank my mom and dad for their unlimited love and attention. I thank them for giving me the privilege to pursue graduate studies in the U.S, for being there for me through all my triumphs and struggles, and for encouraging me always. Lastly, I would like to thank God, and my friend Joy, and also Sisters Theresa, Kathleen, Jean, and Sharon for always loving me and praying for me. Very lastly, I would like to thank my aunt Jeesook and her husband Kihwan Lee for their kindness and warm care while I was with them for my last month at Chicago.

LIST OF ABBREVIATIONS

ADP, adenosine diphosphate

ATP, adenosine triphosphate

BDNF, brain-derived neurotrophic factor

dFMRP, *Drosophila* homologue of the fragile X mental retardation protein

dsRNA, double-stranded RNA

DHC, dynein heavy chain

DIC, differential interference contrast

EGFP, enhanced green fluorescent protein

FEZ1, fasciculation and elongation protein zeta 1

FIONA, fluorescence imaging with one nanometer accuracy

FRAP, fluorescence recovery after photobleaching

FRET, Fluorescence Resonance Energy Transfer

JIP1, c-Jun N-terminal kinase–interacting protein 1

KHC, kinesin heavy chain

KLC, kinesin light chain

mRFP, monomeric red fluorescent protein

MTOC, microtubule organizing center

mRNP, messenger RNA-protein

RNAi, RNA interference

TIRF, total internal reflection microscopy

UTR, untranslated region

TABLE OF CONTENTS

CHAPTER 1: INTRODUCTION	10
1.1 Organelle transport requires activity of motor proteins: kinesin, dynein, and myosin.....	11
1.2 Dynactin is an adaptor protein which interacts with motors, cargo, and microtubules.....	15
1.3 Microtubule transport is important for diverse cellular procedures.	17
1.4 Drosophila S2 cells – a model system to study microtubule-based transport in vivo	18
CHAPTER 2: PEROXISOME TRANSPORT BY KINESIN AND DYNEIN AND 8 nm of IN VIVO PEROXISOME STEPS	20
2.1 SUMMARY	20
2.2 INTRODUCTION	21
2.3 RESULTS	22
2.3.1 Cytochalasin D-induced microtubules in S2 cell processes have a uniform polarity.....	22
2.3.2 Kinesin-1 and cytoplasmic dynein are required for peroxisome transport..	25
2.3.3 Depletion of kinesin-1 or dynein inhibits transport in both directions.....	28
2.3.4 The <i>in vivo</i> average step-size of kinesin-1 and dynein is 8 nm.....	30
2.4 DISCUSSION	32
CHAPTER 3: THE ROLE OF MICROTUBULE BINDING BY DYNACTIN FOR CARGO TRANSPORT AND MICROTUBULE ORGANIZATION	34
3.1 SUMMARY	34
3.2 INTRODUCTION	35
3.3 RESULTS	36
3.3.1 Dynactin is required for bidirectional cargo transport.....	36
3.3.2 Generation of p150 ^{glued} cell lines and RNAi procedure	40
3.3.3 ΔN- p150 ^{glued} forms dynein-dynactin complex.	42
3.3.4 Microtubule binding depends on the N-terminal domain of p150 ^{glued}	44
3.3.5 Dynactin interaction with microtubules is not required for cargo transport.	46
3.3.6 Dynactin binding to microtubules suppresses the generation of multipolar spindles and free microtubule-organizing centers.....	51
3.4 DISCUSSION	53

	7
CHAPTER 4: MICROTUBULE MOVEMENT <i>IN VIVO</i> BY KINESIN-1	57
4.1 SUMMARY	57
4.2 RESULTS	58
4.2.1 Microtubules are highly motile in S2 cells.	58
4.2.2 The suppression of microtubule dynamics (the process of polymerization or depolymerization) does not affect microtubule movement.	59
4.2.3 Generation of stable cells expressing photoconvertible tubulin.	60
4.2.4 Kinesin-1 transports microtubules in S2 cells.	63
4.2.5 Mechanism of kinesin-1-driven microtubule movement.	64
4.3 DISCUSSION	68
CHAPTER 5: CONCLUSION	70
CHAPTER 6: MATERIALS AND METHODS	73
6.1 Molecular cloning	73
6.2 Cell culture	73
6.3. Double-stranded RNAi	75
6.4 Antibodies	75
6.5 Immunofluorescent Staining	76
6.6 Immunoprecipitation	76
6.7 Microscopy and Image Analysis	77
6.8. Sucrose density gradient centrifugation	78
6.9 Microtubule pelleting assay	78
REFERENCES	79
CURRICULUM VITAE	87

LIST OF FIGURES

Figure 1.1. A diagram of a cell, showing the radial organization of the microtubule cytoskeleton and various cargoes	13
Figure 1.2. Structures of conventional kinesin, cytoplasmic dynein, and myosin V.....	13
Figure 1.3. A schematic illustration of the structural features of dynactin subunits	16
Figure 2.1. The morphology of Drosophila S2 cells	23
Figure 2.2. Phase-contrast (A) and fluorescent (B) images of a S2 cell expressing EGFP-tagged peroxisomes in the presence of cytochalasin D. (C) Frames from a time-lapse movie show bidirectional movement of peroxisomes.....	23
Figure 2.3. The polarity of microtubules in S2 processes.....	24
Figure 2.4. Distributions of run lengths (A) and velocities (B) of moving peroxisomes after knock-down of several motors.	26
Figure 2.5. Depletion of cytoplasmic dynein or kinesin stops peroxisome movement.....	27
Figure 2.6. Depletion of one motor (kinesin or dynein) does not deplete the other motor of opposite polarity in both cell extracts and the organelle fraction.	29
Figure 2.7. In vivo imaging of EGFP-peroxisomes in an S2 cell using the FIONA technique.	30
Figure 2.8. Step-by-step movements of peroxisomes	31
Figure 3.1. Dynactin and dynein are required for bidirectional movement of peroxisomes and dFMRP particles.....	38
Figure 3.2. Kinesin can interact with dynein, but not with dynactin.....	39
Figure 3.3. Western blots of extracts of S2 cells expressing mRFP-p150glued or mRFP-ΔN-p150glued.	41
Figure 3.4. Truncated form of p150glued, ΔN-p150glued, forms dynactin complex and interacts with cytoplasmic dynein.	43
Figure 3.5. Truncation of the first 200 amino acid residues of p150glued eliminates microtubule binding.	45

Figure 3.6. Deletion of the microtubule-binding domain of p150glued has no effect on average run length (A) or relative number of runs (B) of both peroxisomes and dFMRP particles.....	47
Figure 3.7. (A) Deletion of the microtubule-binding domain of p150glued has no effect on average velocity of peroxisome or dFMRP particle.....	50
(B) Deletion of the microtubule-binding domain of p150glued has no effect on average run length (B1), relative number of runs (B2), or average velocity (B3) of both endosomes and lysosomes.....	50
(C) The steady-state distribution of peroxisomes, lysosomes, and endosomes in S2 cells expressing wild type p150glued, EGFP-p150glued, or EGFP-ΔN-p150glued.....	50
Figure 3.8. Replacement of p150glued with EGFP-ΔN-p150glued results in the accumulation of multipolar spindles and non-spindle associated (free) MTOCs.....	52
Figure 4.1. The microtubules in the S2 cell cytoplasm are highly motile and keep sliding and looping.	58
Figure 4.2. The treatment of Taxol inhibits the localization of GFP-tagged EB1 protein to tips of microtubules.....	59
Figure 4.3. Photoconversion of Dendra2-tagged tubulin in a S2 cell.	60
Figure 4.4. Fluorescent images of a S2 cell expressing Dendra2-tubulin after photoconversion	62
Figure 4.5. A speed distribution of motile microtubules.	62
Figure 4.6. A diagram showing the relative number of motile microtubules after knock-down of several motor or adaptor proteins.....	64
Figure 4.7. (A) Design of a kinesin mutant where four positively-charged residues in the C-terminal microtubule-binding region were replaced with alanine residues (K925A R929A H932A R936A, Mut-A) (B) The mechanism of microtubule transport by kinesin-1 (C) The examination of kinesin expression levels by Western blot analysis.....	66
Figure 4.8. Effect of mutant kinesin on organelle and microtubule motility.	67
Figure 4.9. A time-lapse movie showing the effect of mutant kinesin on microtubule movements	67

CHAPTER 1: INTRODUCTION

The following dissertation summarizes research conducted at the University of Illinois at Urbana-Champaign and Northwestern University, Feinberg School of Medicine. The main purpose of this study was to understand the mechanism of microtubule-dependent organelle transport in *Drosophila* S2 cells *in vivo*. This work is related to the cytoskeleton, more precisely microtubules and kinesin and dynein motor proteins.

The dissertation begins with Chapter 1, an introduction to intracellular transport, molecular motor, and adaptor proteins; and a brief description of *Drosophila* S2 cells as a model system. The results in Chapter 2 were obtained in collaboration with Comert Kural in the lab of Dr. Paul R. Selvin at the University of Illinois at Urbana-Champaign. This chapter describes an *in vivo* stepping analysis of peroxisomes by using the FIONA technique.

The results in Chapter 3 were obtained in collaboration with Dr. Shuo-Chien Ling in the lab of Dr. Vladimir Gelfand, Dr. Gregory Rogers in the lab of Dr. Stephen Rogers at the University of North Carolina, at Chapel Hill. This chapter explores the role of dynactin on microtubule-dependent transport, especially the role of the microtubule binding domain of the p150^{glued} subunit of the dynactin complex.

Chapter 4 describes microtubule movement and its possible mechanism. In Chapter 5, the dissertation concludes with a summary of this research, as well as a discussion of future studies to enhance our understanding of microtubule-based transport.

Eukaryotic cells distribute intracellular organelles and mRNA and protein complexes in a spatially and temporally regulated manner. Transport along the cytoskeleton system is required for the faithful division of genetic and cellular components during mitosis and cytokinesis. Transport systems are also required for the uptake of extracellular signaling components and for secretion of intracellular components. Therefore, the characterization of the proteins and regulatory mechanisms involved in this transport system plays an important role in understanding fundamental cellular processes.

1.1 Organelle transport requires activity of motor proteins: kinesin, dynein, and myosin

Most transport in eukaryotic cells is driven by three classes of motor proteins: kinesin, cytoplasmic dynein, and myosin (Mallik and Gross, 2004; Schliwa and Woehlke, 2003). Transport occurs along two sets of tracks; actin filaments used by myosins, and microtubules used by both kinesins and dyneins. Microtubules are polar and organized with minus ends at the microtubule organizing center (MTOC) near the nucleus, while the microtubule plus ends are radially arrayed towards cell periphery (Fig 1.1). Most kinesins move toward the plus-ends of microtubules, while dynein moves toward the minus-ends of microtubules. Actin filaments are also polar and their barbed (plus)-ends are oriented to the cell periphery, where they are involved in local membrane traffic such as endocytosis, exocytosis and recycling (Soldati and Schliwa, 2006).

Motors bind to cargo through their tail domains and walk with their heads (motor domain). The kinesin and myosin motors walk by coordinating binding and unbinding of their two heads using energy from hydrolysis of ATP. Many molecular motors are dimers with two

heads connected through coiled-coil domains in a stalk (Fig 1.2). Single-molecule *in vitro* studies have shown that conventional kinesin (kinesin-1), cytoplasmic dynein, and myosin-V are processive motors; they go through repeated ATPase enzyme cycles without getting released from the filaments (Hackney, 1995; King and Schroer, 2000; Mehta et al., 1999; Reck-Peterson et al., 2006).

Both kinesin-1 and myosin-V move by a ‘hand-over-hand’ mechanism, where the ATP/ADP status of the head determines the binding affinity of the head to the filaments and two heads alternate rear and forward positions. The step sizes of kinesin-1 and myosin-V are 8 nm and 36 nm, respectively (Yildiz et al., 2003; Yildiz et al., 2004a).

When kinesin-1 is not bound to a cargo, the motor’s tail domain can fold back onto its head, resulting in the blocking of ATPase activity through a ‘self-inhibition’ mechanism (Coy et al., 1999). A function of the kinesin light chain (KLC) is to keep the kinesin heavy chain (KHC) in an inactive ground state by inducing an interaction between the tail and motor domains of KHC (Verhey et al., 1998). Kinesin-1 motor activity can be regulated by two binding partners, c-Jun N-terminal kinase–Interacting Protein 1 (JIP1) and Fasciculation and Elongation protein ζ Zeta 1 (FEZ1) (Blasius et al., 2007; Verhey et al., 2001). However, the exact regulatory mechanism is not known.

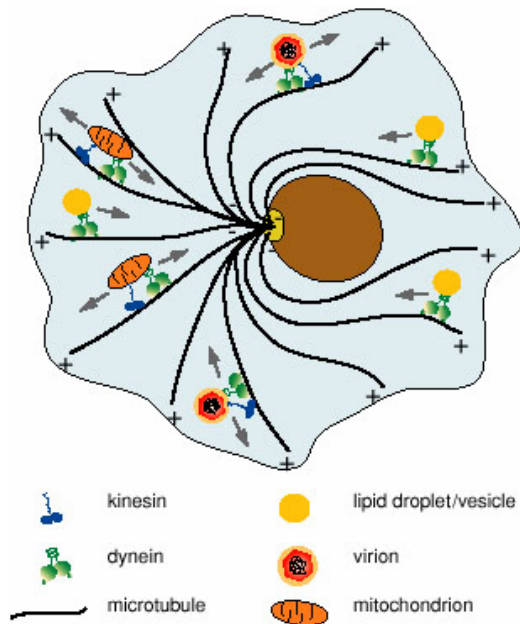


Figure 1.1. A diagram of a cell, showing the radial organization of the microtubule cytoskeleton and various cargoes, namely, lipid droplet/vesicles, virion, mitochondria, etc. which move along microtubules bi-directionally (Gross, 2004).

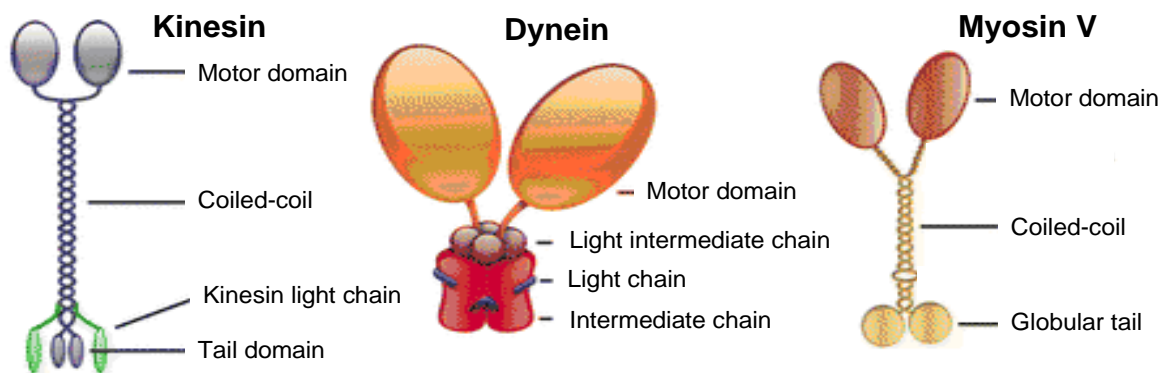


Figure 1.2. Structures of conventional kinesin, cytoplasmic dynein, and myosin V.

Conventional kinesin, cytoplasmic dynein, and myosin V form a dimer through their coiled-coil stalk domain. The motor domains contain binding sites for cytoskeleton and nucleotide. The coiled-coil domain connects the motor domain to the tail domain. Kinesin light chain (KLC) binds through the globular tail domain of kinesin heavy chain (KHC) as shown in green. Dynein complex also has accessory subunits, termed light intermediate chains, light chains, and intermediate chains (courtesy of Roland J. in Dr. Gelfand lab).

Dynein can be classified into two forms: axonemal and cytoplasmic dyneins.

Axonemal dynein functions in bending of cilia and flagella in eukaryotic cells while cytoplasmic dynein is a transport motor and displays diverse roles during mitosis, axonal transport, maintenance of Golgi, and transport of cellular organelles (Holzbaur and Vallee, 1994; Vallee et al., 2004). As shown in Fig 1.2, cytoplasmic dynein contains a homodimer of two heavy chains responsible for ATPase enzymatic activity, and various accessory subunits; intermediate chain (IC), light intermediate chain (LIC), and light chains (LC) – a massive complex almost 10 times bigger than kinesin.

Unlike kinesin and myosin, dynein belongs to the AAA (ATPase associated with diverse cellular activities) class of proteins. The C-terminal portion of the dynein heavy chain (DHC) contains six AAA ATPase domains arranged in a ring structure which has multiple globular domains with ATP binding sites and a stalk outward from the middle of the ring for microtubule binding. All of the accessory subunits are associated with the N-terminal portion of the DHC, which constitutes the base of the dynein. Like kinesin-1, dynein moves in 8 nm steps processively through alternating its rear and forward motor domains. However, dynein has also shown to have variable step sizes and diffusional components in its step: side and backward steps (Gennerich et al., 2007; Reck-Peterson et al., 2006).

Intermediated chains (IC) in *Drosophila* are represented by at least 10 isoforms by alternative splicing in a tissue-specific manner (Nurminsky et al., 1998), suggesting that the regulation of dynein binding to specific organelles occurs through different IC isoforms recruited in dynein complex.

Much of our current understanding of how motors function comes from *in vitro* studies. Based on the above information of motors, in Chapter 2 we will discuss about *in vivo* function of

kinesin and dynein; what is their step-size during *in vivo* organelle transport and how the depletion of either kinesin or dynein affects on bidirectional organelle transport.

1.2 Dynactin is an adaptor protein which interacts with motors, cargo, and microtubules.

A number of adaptor proteins essential for binding motors to cargo have been described recently (Fukuda et al., 2002; Kamal and Goldstein, 2002; Karcher et al., 2002; Wu et al., 2002). Dynactin is a multisubunit complex and has been shown to interact directly with cytoplasmic dynein (Vaughan and Vallee, 1995). Genetic studies in yeast, filamentous fungi, and fly suggest that cytoplasmic dynein and dynactin function in the same cellular pathways (Boylan et al., 2000; Bruno et al., 1996; Holleran et al., 1998).

The main function of dynactin is to attach cytoplasmic dynein to its cargo (Karki and Holzbaaur, 1995; Schroer, 2004; Vaughan and Vallee, 1995). In addition, dynactin has been shown to function as an adaptor for at least two motors of the kinesin family: heterotrimeric kinesin-2 (Deacon et al., 2003) and mitotic kinesin Eg-5 (Blangy et al., 1997). Dynactin also acts independently of cytoplasmic dynein to anchor microtubules at the centrosome (Quintyne et al., 1999; Quintyne and Schroer, 2002). Dynein-dynactin complex plays a role in organizing radial microtubule arrays (Askham et al., 2002). Subcellular localization studies have shown that dynactin is localized at centrosomes and accumulates at the plus ends of microtubules and also on the surface of organelles.

The dynactin complex consists of two morphologically distinct structural domains (Fig 1.3): a rod-shaped domain that binds to the cargo, and an extended projection that mediates an interaction with cytoplasmic dynein and microtubules. The rod-shaped part consists of an Arp-1

filament and actin-capping proteins, while the projection is formed by a homodimer of a p150^{glued} subunit. These two parts of the dynactin complex are bridged by the tetramer of a p50 subunit, dynamitin. p150^{glued} interacts with other subunits of the dynactin complex through its C-terminus and with dynein and other motors through its coiled-coil domains (Schroer, 2004).

Interestingly, p150^{glued} has been shown to bind to microtubules through its N-terminal microtubule binding domain. Microtubule binding by dynactin has been suggested to enhance dynein motor's processivity (King and Schroer, 2000) and also to function at the tips of microtubules by facilitating cargo binding (Vaughan, 2005a). However, the exact mechanism of how the dynactin complex works through microtubule binding is not known. In Chapter 3, we will discuss a role of microtubule binding domain of p150^{glued} on organelle transport and on spindle microtubule organization.

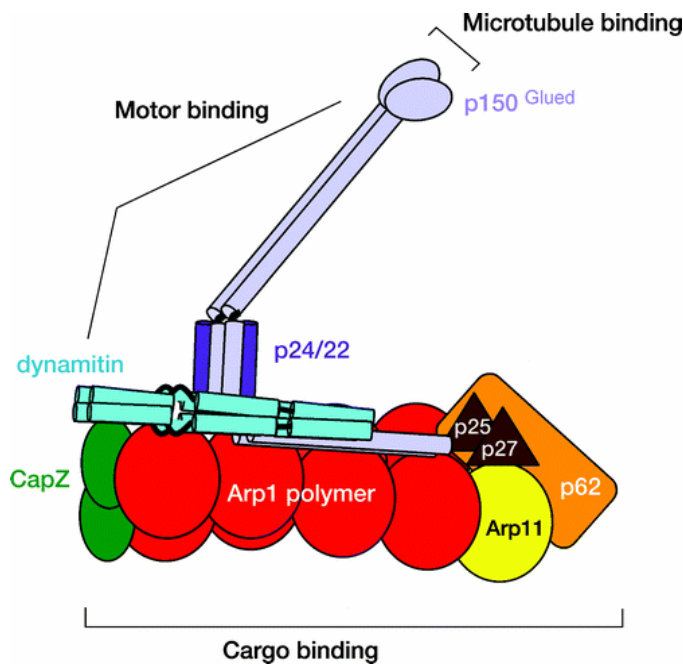


Figure 1.3. A schematic illustration of the structural features of dynactin subunits (Schroer, 2004).

1.3 Microtubule transport is important for diverse cellular procedures.

Microtubule transport (also called microtubule flux) is extensively studied and well-documented in the mitotic spindle (Maddox et al., 2002; Maddox et al., 2003). Microtubule flux is an important cellular process to segregate chromosomes from metaphase plate to each spindle pole. Flux is generated by the combined effort of two microtubule motors: a tetrameric bipolar motor of kinesin-5 family (such as Eg5) which slides along antiparallel microtubules, and a depolymerizing kinesin, the kinesin-13 family (such as Kif2a) that depolymerizes microtubules at the poles (Brust-Mascher et al., 2004; Miyamoto et al., 2004; Rogers et al., 2004).

Significantly less is known regarding microtubule transport in interphase cells. The well-documented example of transport of cytoplasmic microtubules is the bidirectional movement of short microtubules in the axon of cultured neurons (Baas et al., 2006). The anterograde transport was partially inhibited by dynein depletion, while the retrograde transport was dynein-independent and possibly driven by the kinesin-5 family motors (Ahmad et al., 2006; He et al., 2005; Myers and Baas, 2007). The short mobile microtubules presumably serve two main purposes: delivering tubulin and associated proteins along the axon for incorporation into the axonal cytoskeleton, and acting as nucleating elements (seeds) for the assembly of long microtubules.

Another example of microtubule transport is in epithelial cells. Microtubules in polarized epithelial cells are in linear arrays where microtubules are aligned along the apical-basal axis of the cell. In these arrays, the plus ends of microtubules are located basally, whereas the minus ends are apical. These linear microtubules are formed by three steps: **1)** Release from the centrosome or breakage of pre-existing microtubules. **2)** Transport by motor proteins or

treadmilling to sites of assembly. **3)** Rearranged in cell-type-specific arrays by bundling each other.

We demonstrate in S2 cells that microtubules are motile and sometimes move at speeds of microtubule-dependent motors. Not many studies are done about a contribution from the movement of microtubules tracks on cargo transport. In Chapter 4, we examine the mechanism of how microtubule movement (or sliding) is generated in S2 cells. We show that this movement is induced by kinesin-1, and importantly, does not affect organelle motility powered by microtubule-based motors.

1.4 *Drosophila* S2 cells – a model system to study microtubule-based transport *in vivo*

One of the main accomplishments from this study was to establish *Drosophila* S2 cells as a model system to study microtubule-based organelle transport *in vivo*. This is not a scientific result, but development of the system required significant time and effort. The system has been used in our lab and could be used in other labs for further transport study. The lists below describe advantages of this system and also refer to the specific figures or parts of the thesis where the properties were applied for study and discussed in detail.

1) S2 cells can be easily studied under microscopy because they spread as thin layers when being plated on a substrate coated with Concanavalin-A ([Fig. 2.1](#)).

2) S2 cells form processes which have linear microtubule arrays with “uniform” polarity - plus ends mostly towards the tips of processes- when actin filaments are depolymerized ([Fig. 2.1](#)).

Therefore, the polarity of movements is easily determined. An additional advantage of studying

microtubule-based transport in this condition is that S2 cells have no other cytoskeleton system, actin filaments and intermediate filaments which could affect microtubule-based transport.

3) S2 cells are sensitive to RNAi-mediated gene knock-down.

4) Selecting stable S2 cells expressing proteins tagged with different markers (EGFP-peroxisome targeting signal, mRFP-p150^{glued}, mCherry-tubulin etc.) is easier and faster than in other systems.

5) By RNAi knock-down of an endogenous gene and stable expression of the mutant protein, it is easy to replace wild-type proteins with the mutant protein ([Fig.3.3](#)). This RNAi-mediated gene replacement technique was used to study the role of a specific domain in p150^{glued} and kinesin.

Its experimental detail will be explained in Chapter 3.

6) S2 cells grow rapidly in mass culture and provide large amount of cellular factors for biochemical studies.

CHAPTER 2: PEROXISOME TRANSPORT BY KINESIN AND DYNEIN AND 8 nm of *IN VIVO* PEROXISOME STEPS

(Data presented in this chapter was originally published on June 2005 in *Science*, Vol. 308, pp.1469-1472)

2.1 SUMMARY

In many cell types, organelles move along microtubules in both directions; towards the cell periphery and back to the cell center. We questioned how the motors of opposite polarity, kinesin and dynein, determine directionality and transport the same cargo. Is there any cross-talk between two motors? What happens to transport when one motor is depleted? We tried to answer those questions by examining movements of EGFP-tagged peroxisomes along microtubules in S2 cells.

This study demonstrated that kinesin-1 and dynein are required for peroxisome transport; knock-down of either motor stopped peroxisome movement. To examine how peroxisomes walk in nm-scale steps by both kinesin and dynein, the Fluorescence Imaging with One Nanometer Accuracy (FIONA) technique was used. This technique localizes the position of an EGFP-tagged peroxisome to an accuracy of 1.5 nm in 1.1 msec. The results showed that the average step size of peroxisomes was ~8 nm, and agreed with *in vitro* step size for both kinesin-1 and dynein. Interestingly, the knock-down of kinesin-1 or dynein resulted in the complete inhibition of movements in both directions, indicating organelle transport in either direction needs both kinesin-1 and dynein motors. However, exact mechanism of how two motors communicate with each other to transport the same cargo is not known.

2.2 INTRODUCTION

In vitro studies using optical traps (Vale and Milligan, 2000) and single-molecule fluorescence imaging (Yildiz et al., 2004b) have provided insight into how the microtubule motors work. Kinesin is a highly processive motor that can take hundreds of 8-nm steps before detaching from the microtubule (Svoboda et al., 1993; Yildiz et al., 2004a). Optical trap and *in vitro* motility studies have shown that dynein also has an 8 nm step size (Mallik et al., 2004). A recent single-molecule study using recombinant dynein purified from yeast (Reck-Peterson et al., 2006) showed that dynein moves processively without any associated subunits as mostly 8 nm steps; interestingly, the authors observed longer as well as side and backward steps, which differs from kinesin-1. These studies, however, do not address how kinesin and dynein achieve intracellular bidirectional transport *in vivo*.

Fluorescence Imaging with One Nanometer Accuracy (FIONA) applied in S2 cells allows study of cargo transport mediated by motors with high temporal and spatial resolution. The fundamental idea behind FIONA is described below (CSH Protocols; 2007; P. Selvin).

A fluorophore is placed on a coverslip and excited with total internal reflection (TIR) which gives low background fluorescence. The fluorescence is collected and its intensity is plotted as a function of x and y. The approximate localization is the width of the point spread function (which is simply the wide-field diffraction limit of ~250 nm for visible light) divided by the square root of the total number of photons. With 5,000~10,000 collected photons, the resolution is 2.5 nm or 1.25 nm.

Variables, including the detector and background noise, are generally small, and the limiting factor is the number of photons that the fluorophore emits. Since the number of photons

collected from a single EGFP-peroxisome is extremely large, the center of a peroxisome can be easily determined by using a 2D-Gaussian function algorithm. To collect even more photons from EGFP molecules a high numerical aperture objective (60X, N.A. = 1.4) and an oxygen-scavenging system were used. The study of *in vivo* movements of EGFP-peroxisomes by the FIONA technique using a fast charge-coupled device (CCD) camera captured the nanometer scale stepping behaviors of motors in the nanosecond time resolution.

2.3 RESULTS

2.3.1 Cytochalasin D-induced microtubules in S2 cell processes have a uniform polarity.

S2 cells have round shapes and are spread as thin layers on a substrate coated with Concanavalin-A as shown in [Figure 2.1A](#). To study transport along microtubules without interference from any myosin motor-dependent components, cells were treated with Cytochalasin D. Cytochalasin D is a drug that caps barbed ends of actin filaments, resulting in the disappearance of long filaments. After being treated with Cytochalasin D for overnight, S2 cells form long and thin processes having a length of 5-20 μm and a diameter of 0.5-1 μm as shown in [Figure 2.1B](#). In addition, the treatment eliminated the strong retrograde actin flow in the lamelloplasm which could interfere with the analysis of microtubule-dependent movement. Immunofluorescent staining with an α -tubulin antibody showed that these processes contain linear microtubule bundles ([Fig 2.1C](#)). Previous studies have shown that EGFP-tagged peroxisomes and dFMRP particles (Ling et al., 2004) move bidirectionally in these processes ([Fig 2.2](#)).

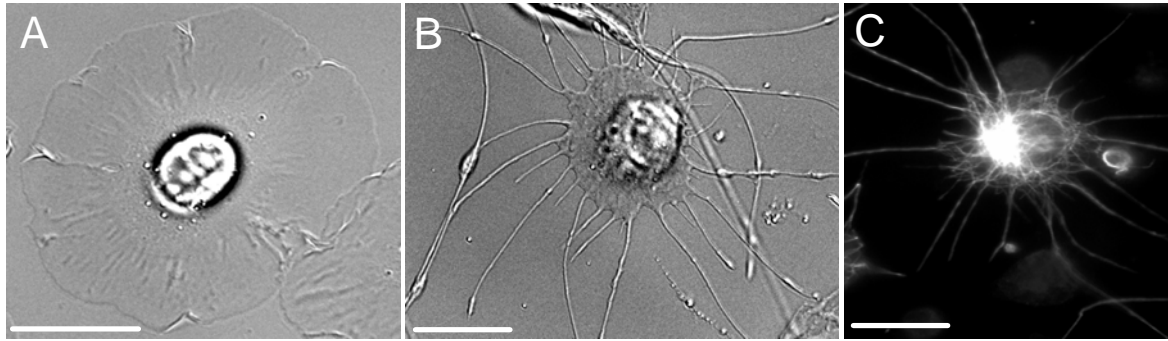


Figure 2.1. The morphology of *Drosophila* S2 cells; (A) a round shape on Concanavalin-A substrate (B) a cell with long and thin processes after incubation with Cytochalasin D, (C) tubulin immunostaining of a cell incubated with Cytochalasin D. Scale bar, 10 μm .

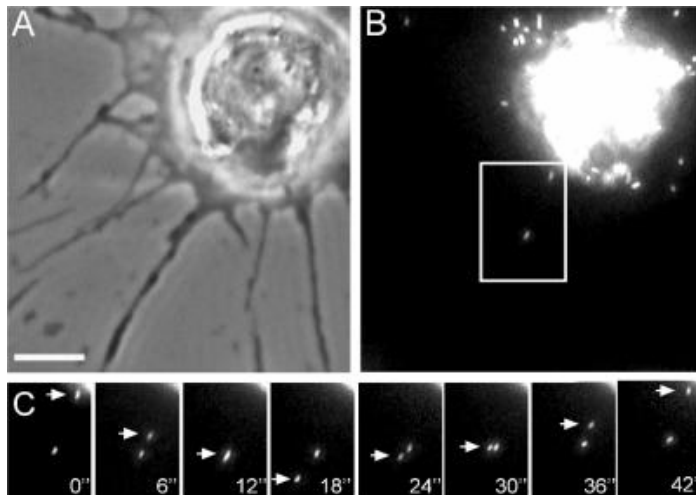


Figure 2.2. Phase-contrast (A) and fluorescent (B) images of a S2 cell expressing EGFP-tagged peroxisomes in the presence of cytochalasin D. (C) Frames from a time-lapse movie show bidirectional movement of peroxisomes. Frames correspond to the boxed area in (B). Time in seconds is indicated on each frame. An arrow shows a peroxisome moving in the process. Scale bar, 5 μm .

This study determined polarity of microtubules in these processes using cells expressing EGFP-tagged EB1 (Fig 2.3). EB1 is a protein that binds to plus ends of growing microtubules, which allowed the determination of where the plus ends of microtubules are present. In thin processes (a diameter less than 1 μm), more than 90% of microtubules have their plus ends towards the tips of processes.

In summary, these preliminary studies demonstrated that Cytochalasin D-induced microtubules in S2 processes have a uniform polarity with their plus-ends toward the tips of the processes and will be used for the rest of our study to determine directionality of transport.

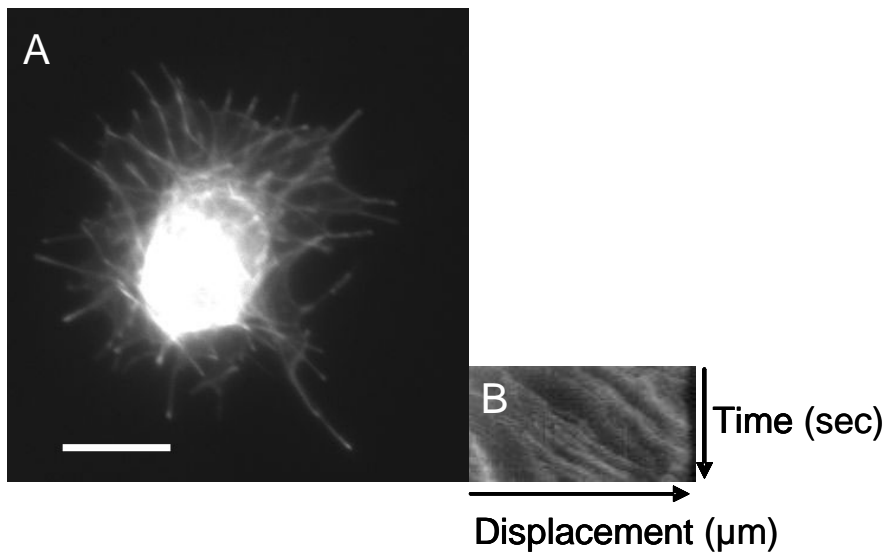


Figure 2.3. The polarity of microtubules in S2 processes. (A) Distribution of EGFP-tagged EB1, microtubule plus tip binding protein, (B) a kymograph showing directional movement of GFP-EB1 towards the tip of the process over time. Scale bar, 10 μm

2.3.2 Kinesin-1 and cytoplasmic dynein are required for peroxisome transport.

Drosophila S2 cells are sensitive to RNAi-mediated gene knock-down. The RNAi technique was used to identify motors which transport peroxisomes along microtubules. Double-stranded (ds)RNA against kinesin-1, kinesin-2 family (Klp68D and Klp64D), kinesin-5 family (Klp61F) or dynein, were treated in the cells expressing EGFP-peroxisomes.

The cells treated with dsRNA against kinesin-1 or cytoplasmic dynein had a significant decrease in peroxisome movement. [Figure 2.4](#) shows a distribution of run lengths (A) or velocities (B) of moving peroxisomes after knock-down of several motors. The average length and velocity of peroxisomes significantly decreased after knock-down of kinesin heavy chain (KHC) or dynein heavy chain (DHC). The relative number of runs of peroxisomes ([Fig 2.5A](#)) also decreased after knock-down of KHC or DHC. The relative number of runs was defined as the number of runs longer than threshold length (2 μ m for peroxisomes) and divided by the total number of particles shown in all frames.

[Figure 2.5B](#) shows KHC or DHC knock-down phenotype of S2 cells expressing EGFP-tagged peroxisomes. The depletion of KHC affected cell morphology and cells treated with dsRNA against KHC generated one thick process in the presence of Cytochalasin D as shown in a DIC (differential interference contrast) image. However, cells treated with dsRNA against DHC generated thin and multiples processes as wild type cells. We do not know the exact mechanism of generating this “KHC knockdown-specific” process. False-colored images (far right) which were merged from first and last frames of time-lapse movies show that the knock-down of kinesin-1 or dynein stopped peroxisome motility in both directions. We conclude that kinesin-1 and dynein are required for peroxisome transport.

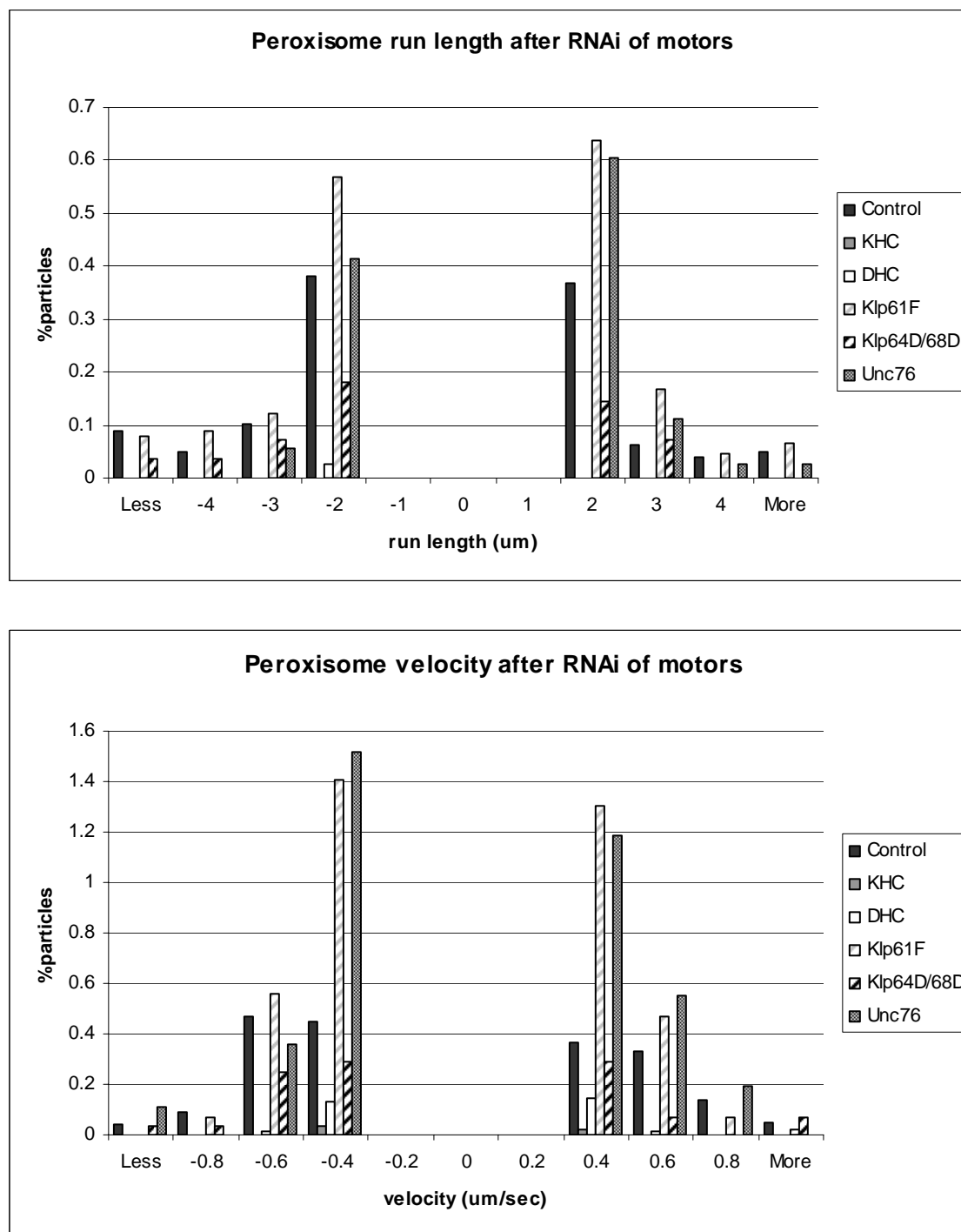


Figure 2.4. Distributions of run lengths (A) and velocities (B) of moving peroxisomes after knock-down of several motors. Note the strong inhibition of motility after knock-down of kinesin heavy chain (KHC) and dynein heavy chain (DHC).

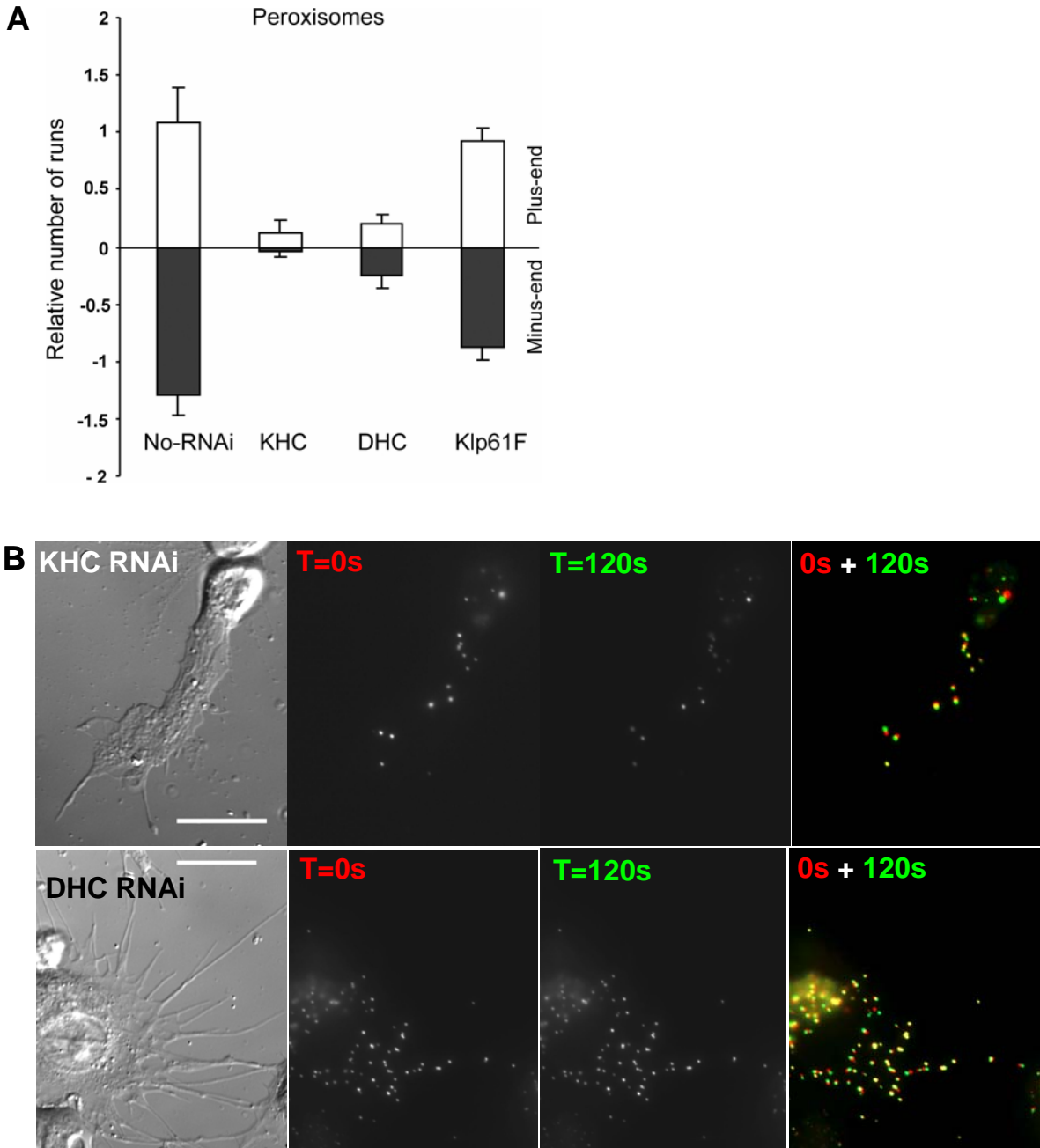


Figure 2.5. Depletion of cytoplasmic dynein or kinesin stops peroxisome movement. (A) The relative number of runs of peroxisomes significantly dropped in both directions after knock-down of kinesin heavy chain (KHC) or dynein heavy chain (DHC). RNAi against a mitotic kinesin Klp61F was used as a control. (B) KHC or DHC knock-down phenotype; a DIC image (far left) and fluorescent images of the same cell. False-colored image (far right) merges two images that span a time interval of 120 sec (T=0 in red; T=120 sec in green). Scale bar, 10 μ m.

2.3.3 Depletion of kinesin-1 or dynein inhibits transport in both directions.

As this study has shown (Fig 2.4 and Fig 2.5), the knock-down of kinesin-1 or dynein decreased peroxisome motility, in both plus and minus directions. These results agreed with previous reports suggesting the coordination of plus- and minus-end directed movement of lipid droplets in *Drosophila* embryos (Gross et al., 2002) and showing an interdependence of dynein, dynactin complex, and kinesin in fast axonal transport in *Drosophila* neurons (Martin et al., 1999). However, the exact mechanism regulating this observed interdependence is not known.

One possible explanation is that the depletion of kinesin (or dynein) causes the release of dynein (or kinesin) on the surface of cargo and results in the inhibition of bidirectional transport simply by the absence of engaged motors on the cargo. To examine the presence of motors after RNAi, cell extracts (soluble fraction) and organelle (membrane) fraction from cells treated with dsRNA against either KHC or DHC, were collected and probed with KHC and DHC antibodies. As shown in Figure 2.6, RNAi-mediated knock-down of kinesin did not affect the level or organelle localization of dynein and *vice versa*, leading to the conclusion that kinesin-1 or dynein alone cannot support peroxisome transport in any direction and that both motors are required for proper organelle transport and localization *in vivo*.

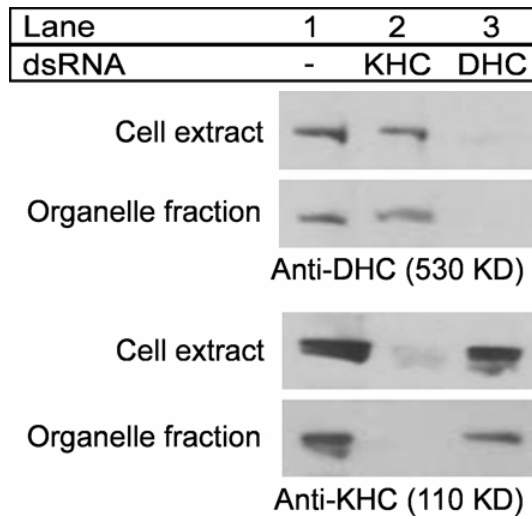


Figure 2.6. Depletion of one motor (kinesin or dynein) does not deplete the other motor of opposite polarity in both cell extracts and the organelle fraction. Lane 1, control cells; Lane 2, cells treated with dsRNA against KHC; Lane 3, cells treated with dsRNA against DHC. Top panel, a blot probed with the DHC antibody; Bottom panel, a blot probed with the KHC antibody.

2.3.4 The *in vivo* average step-size of kinesin-1 and dynein is 8 nm.

The previous studies showed that either kinesin-1 or dynein walks in 8 nm steps *in vitro*, but how both motors walk together to transport cargo *in vivo* is still not known. To study *in vivo* stepping behaviors of peroxisomes by both kinesin-1 and dynein, the FIONA (Park et al., 2007; Yildiz et al., 2003; Yildiz et al., 2004b) technique was used to localize the center of EGFP-peroxisomes. As shown in Fig. 2.7, the fluorescence from an EGFP-peroxisome in a cell process was collected and its intensity was plotted as a function of x and y. The center of the EGFP-peroxisome was determined by using 2D-Gaussian function algorithm.

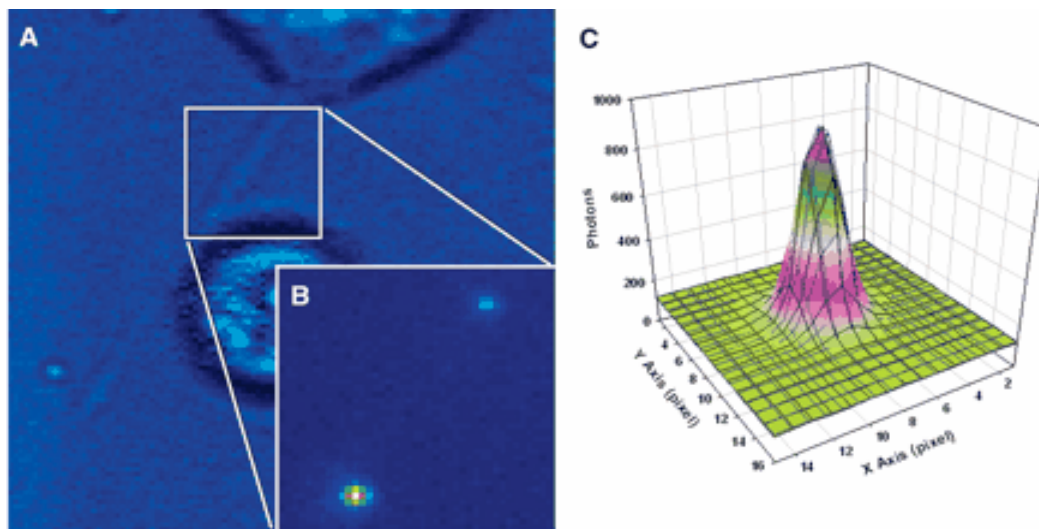


Figure 2.7. In vivo imaging of EGFP-peroxisomes in an S2 cell using the FIONA technique. (A) Bright-field image of a cytochalasin-D-treated S2 cell with a thin process. (B) Fluorescence image of EGFP-labeled peroxisomes (C) The center of the EGFP-peroxisome was determined by using 2D-Gaussian function algorithm.

Figure 2.8 demonstrates the movement of EGFP-peroxisomes in a step-by-step manner in both plus (driven by kinesin) and minus (driven by dynein) directions. The average step size from 169 motor steps in the kinesin direction is 8.6 ± 2.7 nm (mean \pm SD). The average step size from 188 motor steps in the dynein direction is 8.9 ± 2.6 nm. These results are in perfect agreement with *in vitro* step size of kinesin-1 and dynein shown before (Svoboda et al., 1993) (Mallik et al., 2004). We thus conclude that kinesin-1 and dynein transport peroxisomes by taking 8 nm steps and conserving their stepping behaviors on the surface of cargoes *in vivo*.

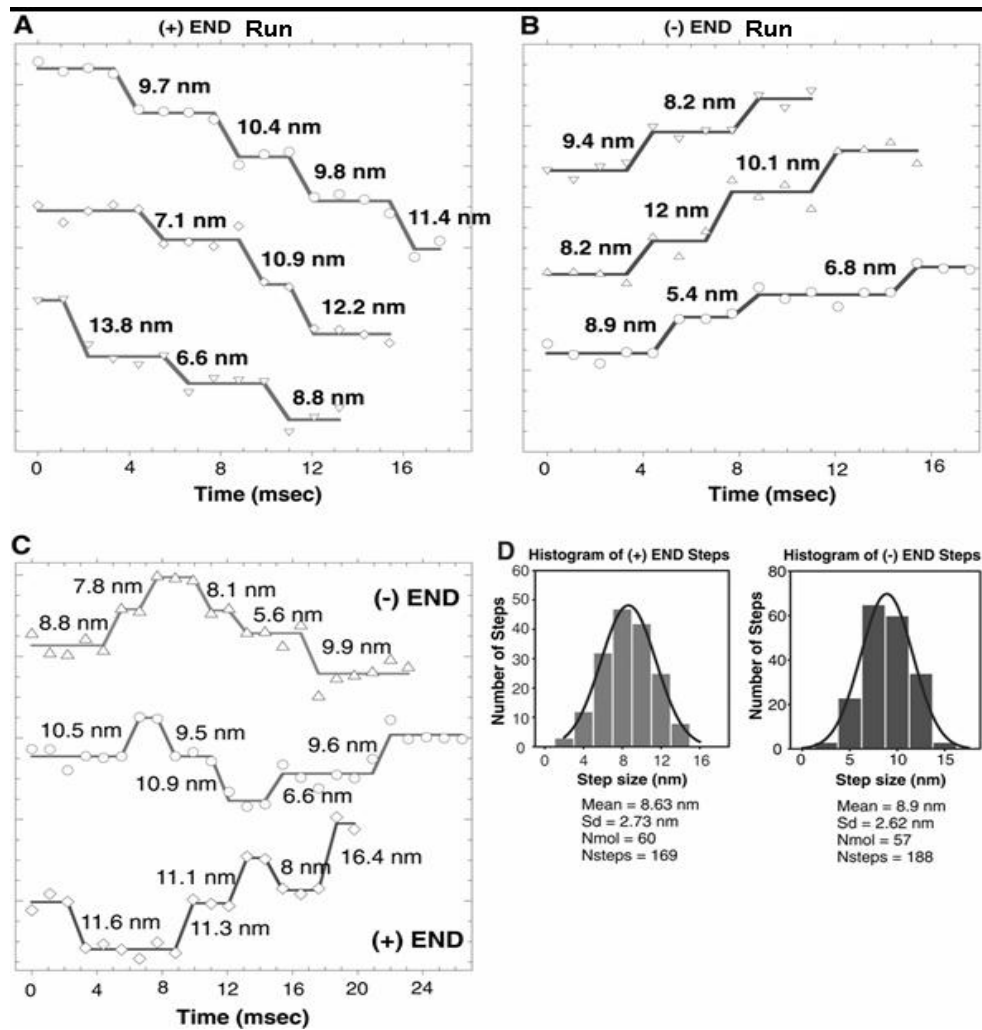


Figure 2.8. Step-by-step movements of peroxisomes driven by (A) kinesin, (B) dynein, and (C) both kinesin and dynein. (D) Histograms of individual steps of plus and minus movements.

2.4 DISCUSSION

This study showed that kinesin-1 and dynein are required for peroxisome transport in S2 cells. FIONA technique demonstrated that peroxisomes walk as 8 nm steps by kinesin-1 and dynein, which is in agreement with *in vitro* step sizes of kinesin-1 and dynein.

Few degenerated steps (less than 8 nm or between 8 or 16 nm) were observed. We assume that these degenerated steps come from the detector or background noise from *in vivo* environment; peroxisomes are in a viscous and dynamic cytoplasm. Since the length of a tubulin dimer is 8 nm, we assume that only one binding site is structurally favored by kinesin and dynein and steps lesser than 8 nm are not possible. However, in the system used by this study, the EGFP signal originated from the center of a huge peroxisome, and not from relatively small individual motors. Therefore, degenerated steps could originate from the deformation (elongated or asymmetric shape) of a peroxisome by a motor stepping 8 nm and being dragged by the opposing motor at the same time if they are in tug-of-war (but, we did see only few degenerate steps indicating that the activities of motors are coordinated by unknown mechanisms). Further tracking of fluorescently labeled motors at FIONA resolution are needed to rule out this possibility.

In addition, Gennerich et al recently showed that high tension (~10 pN) of dragging force on dynein induced frequent backward stepping of less than 8 nm (4 nm) or larger than 8 nm (16 or 24 nm) in studies using *in vitro* beads trapped by optical tweezers (Gennerich et al., 2007). These large steps of dynein were not observed in our study.

This study did not examine the processivity of runs; how many steps kinesin or dynein walks along microtubules without stopping or changing directions. Compared to normal tracking,

the processivity analysis at this resolution (FIONA) would provide the number of steps that kinesin-1 or dynein could walk before it detaches from microtubule tracks by any external forces.

If a dragging force or friction generated by the opposing motor exists, a decrease in continuous unidirectional steps and an increase in directional changes or stationary phase could be expected. Further quantitative analysis at high temporal and spatial resolution is required to address how kinesin-1 and dynein work together to transport the same cargo.

We did not see the phenotype of hyper-aggregation or hyper-dispersion of peroxisomes after RNAi of either kinesin-1 or dynein. Rather, we only observed a complete inhibition of bidirectional transport. This indicates that kinesin-1 or dynein alone cannot support transport in any direction and that both motors are required for proper organelle transport and localization *in vivo*. But, the mechanism regulating these activities is not known.

We do not know how the presence of one motor affects the other motor. The opposing motor may be required for the proper orientation of a motor for its full activity. In future studies, kinesin mutants with reduced ATPase activity, but with the same microtubule binding and cargo interacting activities, could be examined to determine whether they support dynein-driven organelle transport and show a hyper-aggregation phenotype.

CHAPTER 3: THE ROLE OF MICROTUBULE BINDING BY DYNACTIN FOR CARGO TRANSPORT AND MICROTUBULE ORGANIZATION

(Data presented in this chapter was originally published on February, 2007 in *The Journal of Cell Biology*, Vol. 176, pp. 641-651)

3.1 SUMMARY

Dynactin complex functions as an adaptor by linking cytoplasmic dynein and other motors to cargo. The largest subunit of dynactin, p150^{glued}, binds dynein intermediate chain (DIC) through its coiled coil domain and also binds microtubules through N-terminal binding domain. *In vitro* studies have suggested that microtubule binding by p150^{glued} affects motor's processivity by providing an extra binding site for microtubule, but its exact role is not known.

To explore the role of microtubule binding by dynactin, wild-type p150^{glued} in S2 cells was replaced with mutant Δ N-p150^{glued} that lacked residues 1-200, making them unable to bind microtubules. Interestingly, while movement of organelles and mRNP particles absolutely required dynactin, the substitution of full-length p150^{glued} with Δ N- p150^{glued} did not affect the relative number of runs, run length, and velocity of transport. Next, this study examined its role on spindle microtubule organization in mitotic cells. Truncation of the microtubule-binding domain of p150^{glued} had a dramatic effect on cell division, resulting in the generation of multipolar spindles and free microtubule-organizing centers. We conclude that dynactin binding to microtubules is required for organizing spindle microtubule arrays but not for cargo transport *in vivo*.

3.2 INTRODUCTION

Dynactin complex functions as an adaptor by linking cytoplasmic dynein and other motors to cargo. The largest subunit of dynactin, p150^{glued}, binds dynein intermediate chain (DIC) through its coiled coil domain and also binds microtubules through N-terminal binding domain. The microtubule-binding region of p150^{glued} consists of a CAP-Gly domain and a basic-rich domain, both of which are positioned within the first 200 amino acid residues (Culver-Hanlon et al., 2006; Vaughan et al., 2002; Waterman-Storer et al., 1995).

Analysis of p150^{glued} isoforms in mammalian brains showed that in addition to the full-length p150^{glued}, neurons express an alternatively spliced 135-kDa isoform lacking the microtubule-binding domain (Tokito et al., 1996). The p135 isoform was suggested to assemble into distinct dynactin complexes from p150^{glued}, but its exact role is not known. The microtubule binding domain might be dispensable for at least some of the dynactin functions in non-dividing cells.

In vitro motility assays using beads coated with a mixture of cytoplasmic dynein and dynactin demonstrated that dynactin functions as a processivity factor for dynein (King and Schroer, 2000), presumably by providing an extra binding site for microtubules and thus preventing cargo dissociation from microtubules (Culver-Hanlon et al., 2006; Kobayashi et al., 2006; Waterman-Storer et al., 1995).

Another function of the microtubule-binding domain of p150^{glued} is to localize the dynein-dynactin complex to the plus-ends of growing microtubules (Vaughan et al., 2002). p150^{glued} is a family member of microtubule plus end-binding proteins (Akhmanova and Hoogenraad, 2005) and colocalizes with other proteins of this class such as CLIP-170 and EB1

to the plus-ends of growing microtubules (Lansbergen et al., 2004; Ligon et al., 2003; Vaughan et al., 1999). Its binding affinity to microtubules could be regulated by phosphorylation (Vaughan et al., 2002), but its exact mechanism is not known. It has been postulated that the accumulation of p150^{glued} at the plus ends of microtubules facilitates the loading of the retrograde cargo on microtubules (Vaughan, 2005b) and also the linking of microtubule plus-ends to specific sites, such as at mitotic kinetochores or at the cell cortex (Mimori-Kiyosue and Tsukita, 2003).

Both microtubule tip-binding and enhancement of motor processivity by dynactin require the N-terminal microtubule binding domain of p150^{glued}. However, the existence of the shorter p135 isoform of p150^{glued}, which lacks the microtubule-binding domain, suggests that the dynactin complex can perform at least some of its functions even without this microtubule binding activity. Here, we explored the effects of the deletion of the microtubule binding domain on cargo transport and the organization of spindle microtubules.

3.3 RESULTS

3.3.1 Dynactin is required for bidirectional cargo transport.

To investigate the role of dynactin in the process of microtubule-dependent transport, the study used two types of cargo: membranous organelles (peroxisomes, endosomes, and lysosomes) and non-membranous mRNA-protein (mRNP) complexes (*Drosophila* homologue of the Fragile X protein, dFMRP). Both EGFP-tagged peroxisomes and EGFP-tagged dFMRP particles have a well-defined morphology and are transported along microtubules by cytoplasmic

dynein and conventional kinesin (kinesin-1) as demonstrated previously (Kural et al., 2005; Ling et al., 2004).

In order to study the role of dynactin in cargo transport, we knocked down either p150^{glued} or p50-dynamitin subunits of the *Drosophila* dynactin complex. Such treatment effectively reduced bidirectional transport of both types of cargo, demonstrating that dynactin is required not only for transport of membranous organelles but also for transport of mRNP particles along microtubules (Fig 3.1A). RNAi against a mitotic kinesin Klp61F was used as a control. Western blots against DHC and p150^{glued} were shown in Figure 3.1C.

Examination of the database showed that there is a second p150^{glued} gene in *Drosophila* (gi|23093121|gb|AAF49148.2) (Goldstein and Gunawardena, 2000). Additional experiment was done to address whether the existence of the second gene rescues and compensates for loss of the conventional p150^{glued}. RNAi against the second gene did not change organelle movement, either in the wild-type or Δ N-p150^{glued} cells. However, RNAi against the conventional p150^{glued} completely blocked organelle movement. This suggests that the second gene is not important for organelle transport or not even expressed in S2 cells.

To further confirm the role of dynactin in cargo transport, we overexpressed mRFP fusion proteins with either p50-dynamitin or the first coiled-coil region (amino acid residues, 232-583) of p150^{glued}. Both constructs act as dominant negative inhibitors of dynactin-dependent cellular processes (Burkhardt et al., 1997; Quintyne et al., 1999; Waterman-Storer et al., 1997). As shown in Figure 3.1B, overexpression of either protein dramatically inhibited transport of peroxisomes and dFMRP particles.

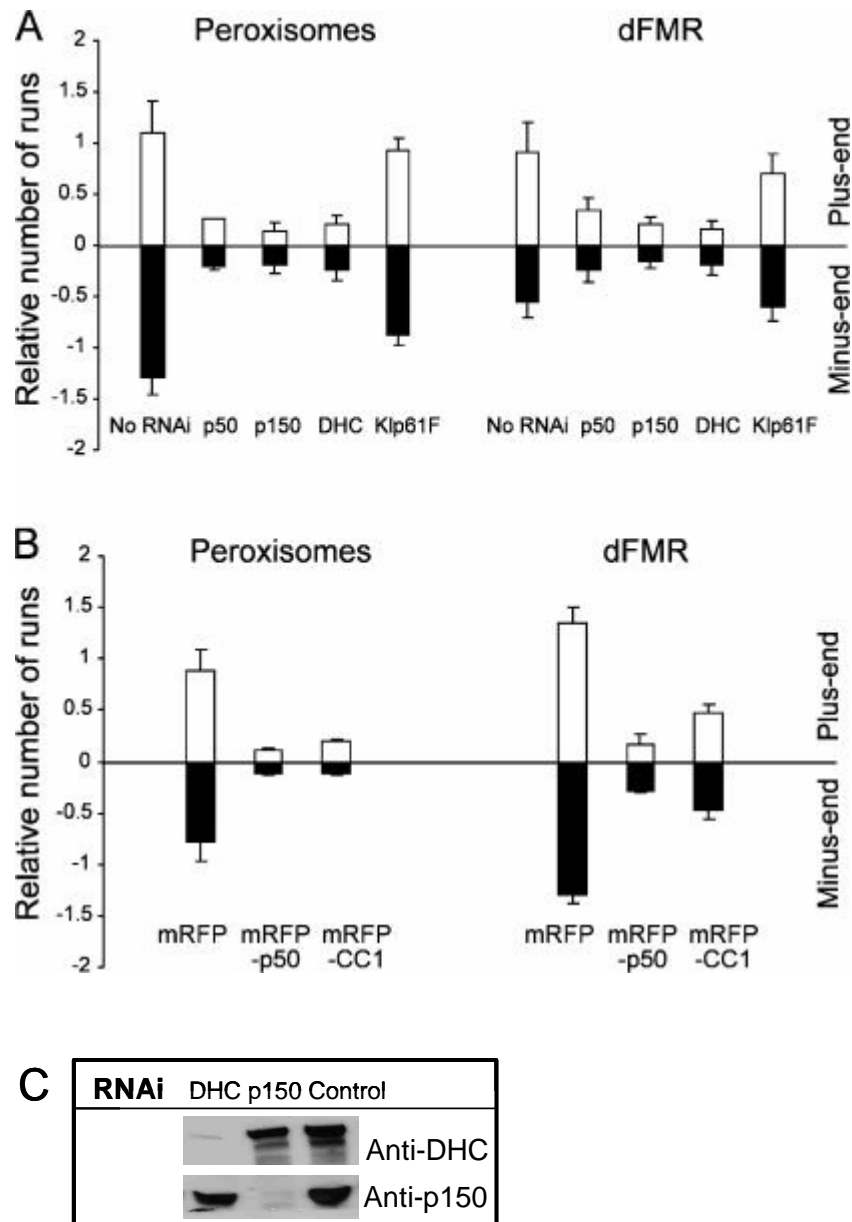


Figure 3.1. Dynactin and dynein are required for bidirectional movement of peroxisomes and dFMRP particles. (A) The relative number of runs (see Materials and Methods) of both peroxisomes and dFMRP particles significantly dropped after knock-down of dynactin subunits (p50 or p150^{glued}) or DHC. RNAi against a mitotic kinesin Klp61F was used as a control. (B) The relative number of runs of both peroxisomes and dFMRP particles significantly dropped after overexpression of dominant negative inhibitors of dynactin, mRFP-p50 or mRFP-tagged coiled-coil 1 of p150^{glued} (mRFP-CC1). (C) Western blots of DHC and p150^{glued} after RNAi.

It is worth noting that as was the case of dynactin knock-down, both the plus- and minus-end movements were inhibited by overexpression of dynactin subunits. Binding of both kinesin and dynein to dynactin could be one potential mechanism of inhibiting bidirectional transport in cells that are either depleted of dynactin subunits or overexpressing dominant-negative dynactin constructs. Immunoprecipitation assays were performed to address this possibility. An antibody against p150^{glued} pulled down DHC, but not KHC from S2 extracts. Similarly, a KHC antibody did not pull down p150^{glued}, although, in agreement with a previous report (Ligon et al., 2004), it pulled down DHC (Fig 3.2). Thus, we conclude that dynactin is required for bidirectional transport but may not bind simultaneously to the two opposing motors to regulate their activities. Other proteins and/or direct interactions between kinesin and dynein possibly play a role in regulating motor activities.

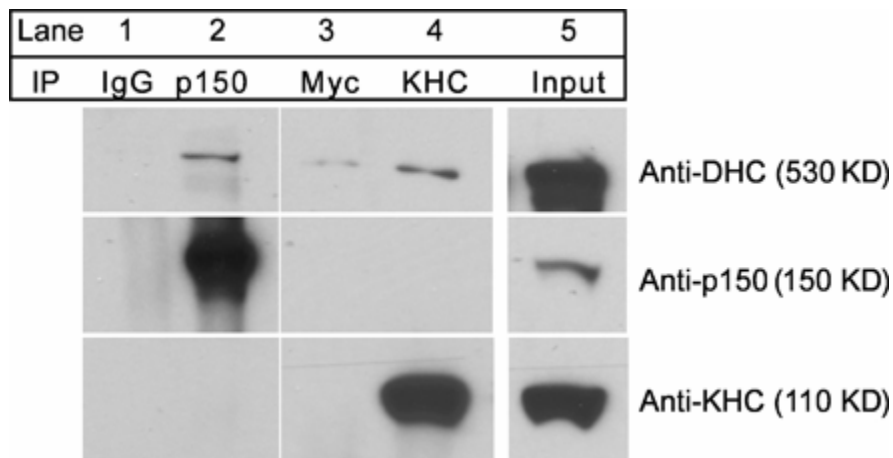


Figure 3.2. Kinesin can interact with dynein, but not with dynactin. An antibody against p150^{glued} pulled down DHC, but not KHC from S2 extracts (lane 2). Similarly, an antibody against KHC did not pull down p150^{glued} although it did pull down DHC (lane 4). Normal rabbit IgG and anti-Myc antibody were used as controls (lane 1, 3).

3.3.2 Generation of p150^{glued} cell lines and RNAi procedure

To replace the wild-type p150^{glued} with a truncated form, we generated S2 cell lines expressing a fusion protein of monomeric red fluorescent protein (mRFP) or EGFP with the N-terminus of either full-length p150^{glued} or p150^{glued} with a deletion of residues 1-200 (Δ N-p150^{glued}). Stable cell lines were selected by hygromycin and then the cells were treated with dsRNA corresponding to the 3'-untranslated region (UTR) of p150^{glued} mRNA to deplete the endogenous protein.

Western blotting with an antibody that recognizes the C-terminal fragment of p150^{glued} showed that, in addition to the endogenous protein, stable cell lines expressed new proteins with molecular weights expected for fusions of either full-length p150^{glued} or Δ N-p150^{glued} tagged with mRFP (Fig 3.3A; lanes 1, 3). The antibody generated against residues 1-200 of p150^{glued} did not recognize Δ N-p150^{glued} (Fig 3.3A, lane 7) demonstrating that the construct indeed lacked its N-terminus.

As mentioned above, to deplete endogenous p150^{glued}, we treated cells with a dsRNA corresponding to the 3'-untranslated region (UTR) of p150^{glued} mRNA. As shown in Figure 3.3A (lanes 2, 4, 6, 8) such treatment dramatically reduced the levels of endogenous p150^{glued} but did not affect the expression of mRFP-tagged p150 fusion proteins, as mRNAs encoding these proteins do not have the 3'-UTR region. Thus, by combining the stable expression of tagged p150^{glued} constructs and the RNAi-mediated knock-down of the endogenous p150^{glued}, the endogenous protein can be replaced with tagged p150^{glued} or Δ N-p150^{glued} protein. Figure 3.3B shows a diagram of the gene replacement technique described above.

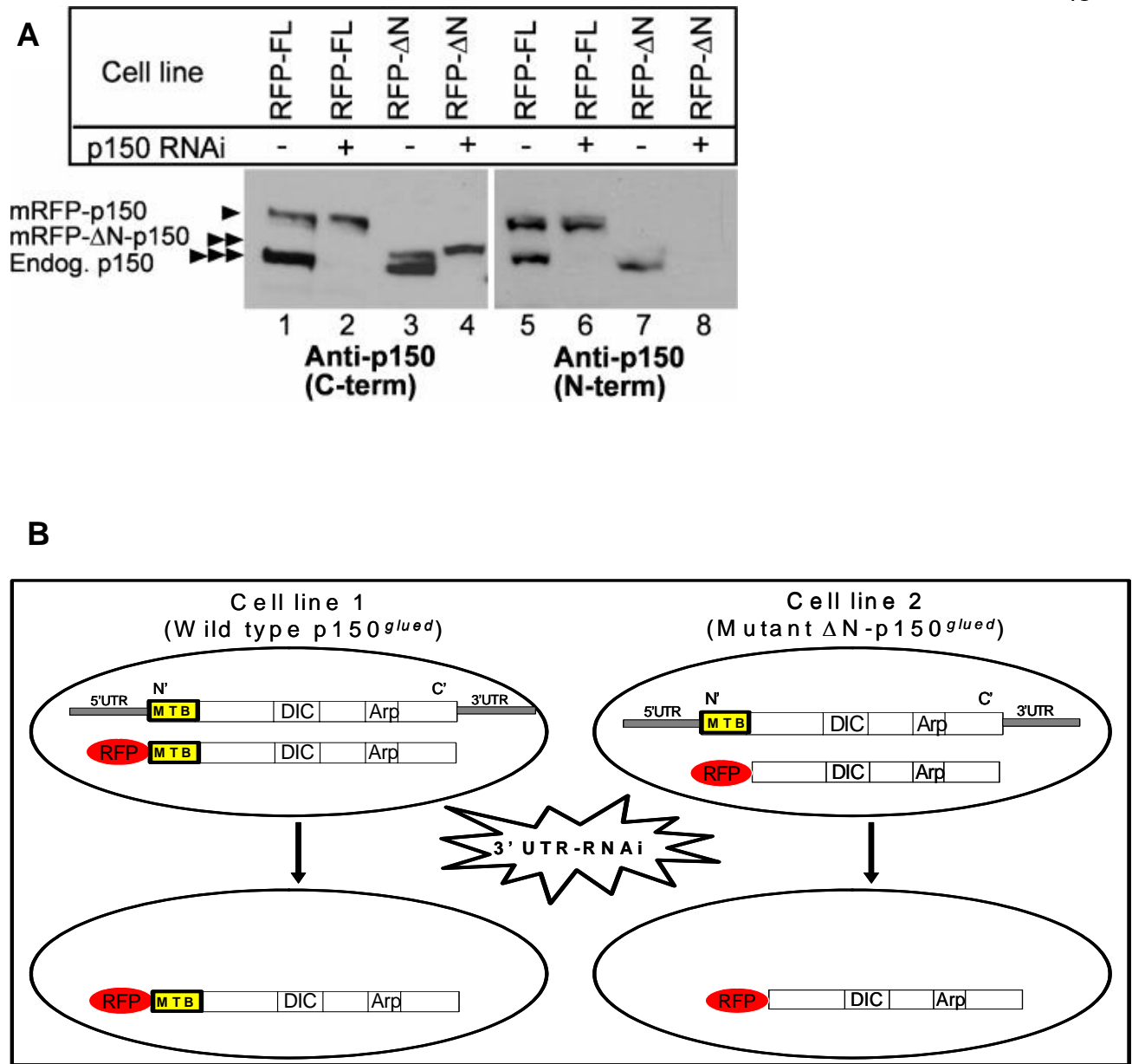


Figure 3.3. (A) Western blots of extracts of S2 cells expressing mRFP-p150^{glued} (lanes 1, 2, 5, 6) or mRFP-ΔN-p150^{glued} (lanes 3, 4, 7, 8). Endogenous p150^{glued} was depleted by using RNAi against the 3'-UTR of p150^{glued} mRNA (lanes 2, 4, 6 and 8). Lanes 1-4 were probed with an antibody against C-terminal fragment of p150^{glued}, and lanes 5-8 were probed with an antibody against N-terminal fragment of p150^{glued}. Positions of mRFP-p150^{glued}, mRFP-ΔN-p150^{glued} and endogenous p150^{glued} bands are marked by single, double and triple arrowheads, respectively. (B) A diagram showing the gene replacement technique

3.3.3 ΔN -p150^{glued} forms dynein-dynactin complex.

To examine whether truncation of the microtubule-binding domain affects the ability of p150^{glued} to form a dynactin complex and to interact with dynein, we analyzed the sedimentation behavior of dynein-dynactin complex in sucrose density gradients. Wild-type S2 cells and cells expressing EGFP-p150^{glued} or EGFP- ΔN -p150^{glued} were used and endogenous p150^{glued} was depleted by RNAi. To monitor sedimentation behavior of p150^{glued}, gradient fractions were probed with an N-terminal p150^{glued} antibody (untransfected cells) or an EGFP-antibody (transfected cells). Dynein in gradient fractions was probed using DHC antibody.

Western blot analysis of the fractions demonstrated that endogenous p150^{glued}, EGFP-p150^{glued} and EGFP- ΔN -p150^{glued} have identical sedimentation profiles in sucrose gradients with a peak that coincides with the peak of cytoplasmic dynein (Fig 3.4A). Kinesin heavy chain (KHC) was probed for as a control protein that does not sediment with DHC. These results indicate that neither truncation of the microtubule-binding domain nor fusion with EGFP affects the ability of p150^{glued} to incorporate into the dynactin complex.

To further confirm formation of the dynactin complex by ΔN -p150^{glued} and its ability to interact with dynactin complex, an immunoprecipitation assay was performed. EGFP antibody was used to pull down EGFP-p150^{glued} or EGFP- ΔN -p150^{glued} and the precipitates were probed for other dynactin subunits. Figure 3.4B shows that dynactin subunits, p50-dynamitin and Arp1, as well as DHC, were detected in the precipitates with EGFP antibody from both cells expressing EGFP-p150^{glued} or EGFP- ΔN -p150^{glued}, but not from untransfected cells or in precipitates with a preimmune IgG serum. We conclude that ΔN -p150^{glued} incorporates into the dynactin complex and that this complex interacts with cytoplasmic dynein.

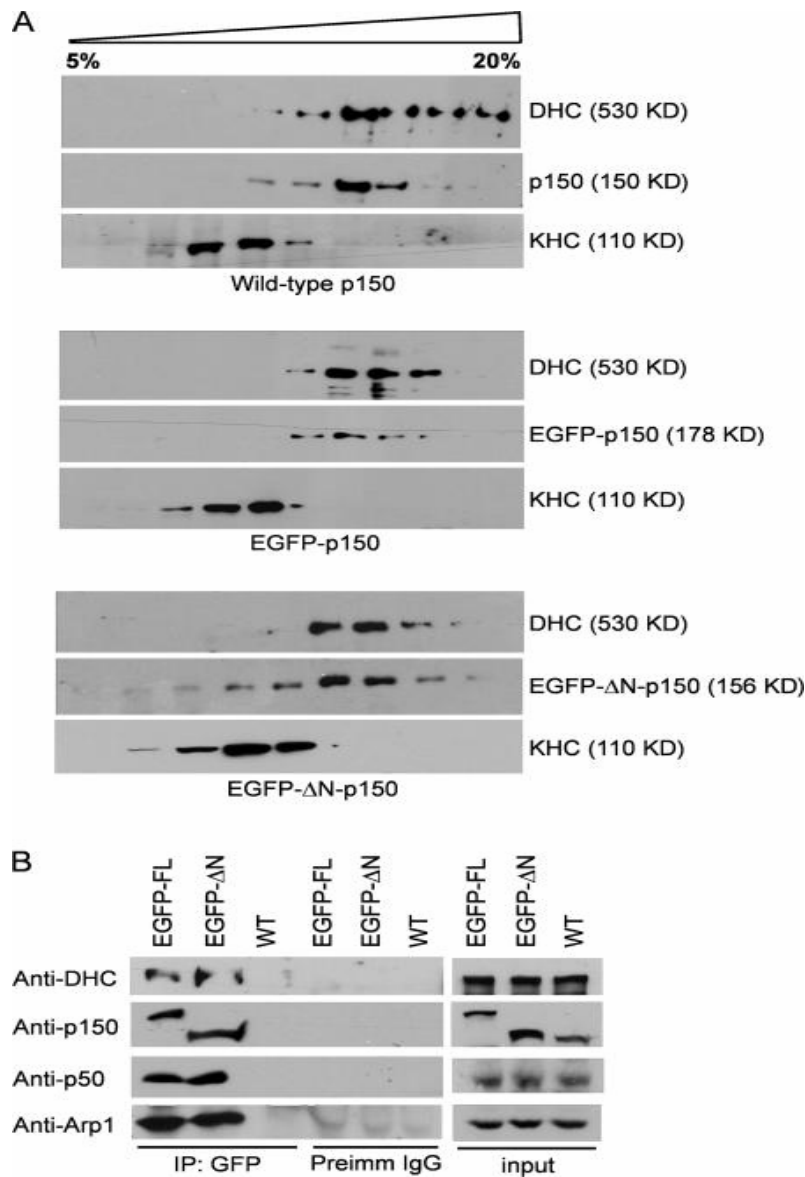


Figure 3.4. Truncated form of p150^{glued}, ΔN-p150^{glued}, forms dynactin complex and interacts with cytoplasmic dynein.

(A) Sucrose gradient fractionation of extracts from S2 cells expressing wild-type p150^{glued}, EGFP-p150^{glued}, or EGFP-ΔN-p150^{glued}. EGFP-ΔN p150^{glued} sediments at the same rate as wild-type p150^{glued} or EGFP-p150^{glued}. **(B)** Extracts from cells expressing EGFP-p150^{glued} or EGFP-ΔN-p150^{glued} and untransfected cells, were immunoprecipitated with an EGFP antibody or control IgG. Precipitates were probed using DHC antibody and antibodies against dynactin subunits p150^{glued}, p50, and Arp-1. Note that EGFP-antibody but not the control IgG pulls down cytoplasmic dynein and dynactin subunits. Inputs are cell extracts from each sample.

3.3.4 Microtubule binding depends on the N-terminal domain of p150^{glued}.

To examine the microtubule binding activity of EGFP-p150^{glued} or EGFP-ΔN-p150^{glued}, we performed a pelleting assay with microtubules *in vitro* and a colocalization study with microtubules in S2 cells.

For microtubule pelleting assays, we expressed recombinant proteins containing either amino acid residues 1-600 or 200-600 of p150^{glued} fused to EGFP and His₆ tags. Both proteins were purified by using a Talon affinity column, incubated with Taxol-stabilized microtubules, and pelleted by centrifugation through a glycerol cushion. As shown in [Figure 3.5A](#), p150^{glued} (1-600) bound to microtubules while truncation of 200 residues from the N-terminus abolished microtubule binding. These results confirm previous reports, which demonstrated that the microtubule binding domain of p150^{glued} are localized within the residues 1-160 of the protein (Culver-Hanlon et al., 2006; Waterman-Storer et al., 1995).

For *in vivo* analysis of microtubule binding, we depleted endogenous p150^{glued} by RNAi and transiently transfected cells with either EGFP-p150^{glued} or EGFP-ΔN-p150^{glued} constructs. Cells were extracted with Triton X-100 to remove soluble proteins, fixed, and double-stained for microtubules and EGFP. As shown in [Figure 3.5B](#), EGFP-p150^{glued} decorated cytoplasmic microtubules. However, EGFP-ΔN-p150^{glued} did not show any microtubule binding. Interestingly, both EGFP-p150^{glued} and EGFP-ΔN-p150^{glued} were found in small clusters in the cytoplasm. The nature of these clusters remains unknown.

Here, we confirm that the first 200 amino acid residues of p150^{glued} contain microtubule-binding activity and the truncation of this domain completely eliminates the ability of p150^{glued} to interact with microtubules.

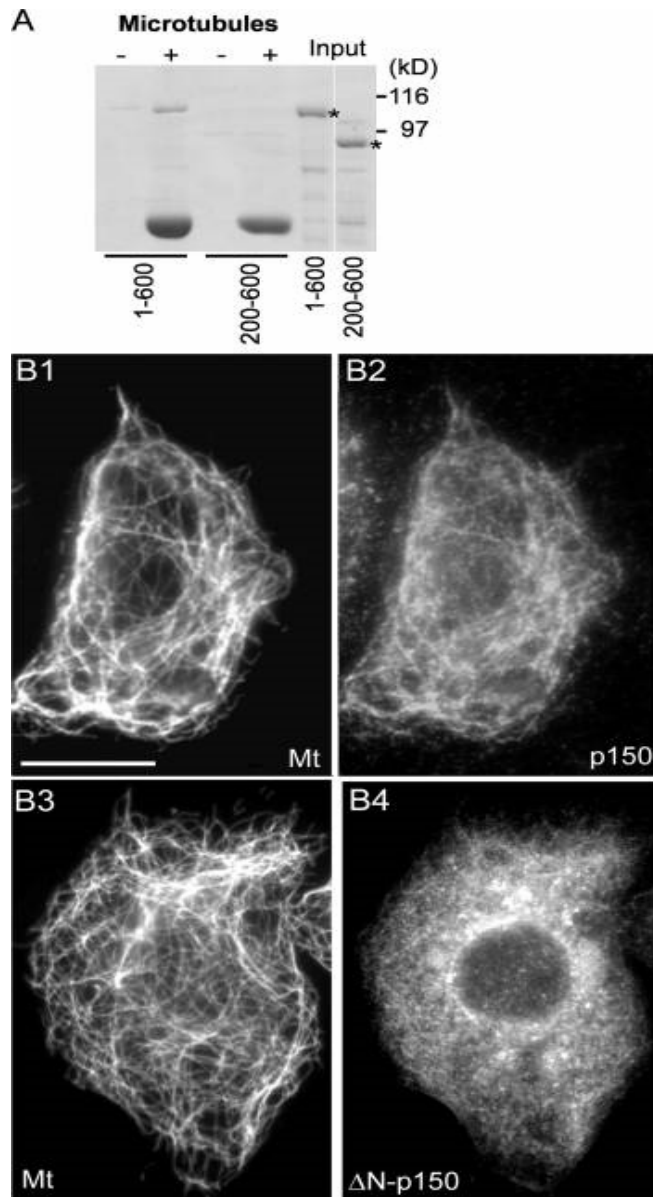


Figure 3.5. Truncation of the first 200 amino acid residues of p150^{glued} eliminates microtubule binding. (A) Recombinant proteins purified and incubated with Taxol-stabilized microtubules were centrifuged to pellet with microtubules. Pellets were analyzed by SDS-gel electrophoresis. Inputs are proteins used for assay and asterisks mark positions of His₆-p150^{glued} (residues 1-600) or His₆-p150^{glued} (residues 200-600). (B) EGFP-tagged p150^{glued} (B2) is aligned along microtubules (B1) and EGFP-ΔN-p150^{glued} (B4) shows no microtubule binding. Cells were treated with 3'UTR RNAi to deplete endogenous p150^{glued}, extracted with detergent and stained with a monoclonal α-tubulin antibody and EGFP-polyclonal antibody. Scale bar, 10 μm.

3.3.5 Dynactin interaction with microtubules is not required for cargo transport.

To determine the role of the microtubule-binding domain of p150^{glued} on microtubule-dependent cargo transport, we analyzed movement of EGFP-tagged peroxisomes and dFMRP particles in S2 cells expressing either mRFP-p150^{glued} or mRFP-ΔN-p150^{glued}. Cells were treated with RNAi against the 3'-UTR of p150^{glued} mRNA to deplete endogenous p150^{glued}. Observation of cargo movement in these cells indicated that replacement of wild-type p150^{glued} with either mRFP-p150^{glued} or mRFP-ΔN-p150^{glued} did not affect peroxisome or dFMRP particle transport. Similar to the wild-type, ΔN-p150^{glued} supported transport of EGFP-labeled cargo in both directions along microtubules, while complete depletion of p150^{glued} did not support the cargo transport.

Quantitative analysis demonstrated that removal of the microtubule-binding domain of p150^{glued} did not affect long-range movement of peroxisomes or dFMRP particles along microtubules. Unlike complete depletion of p150^{glued}, replacement with mRFP-ΔN-p150^{glued} did not affect the average run length and the relative number of runs of either peroxisomes or dFMRP particles (Fig 3.6). The relative number of runs was determined as the number of runs longer than a threshold value, normalized to the number of analyzed particles (see Materials and Methods). This parameter should be most dramatically affected if the processivity of organelle movement was changed. We also compared the average velocity of runs, which was not changed by expressing mRFP-ΔN-p150^{glued} (Fig 3.7A). The motile parameters observed here clearly addressed that peroxisome and dFMRP transport was not affected by the removal of the microtubule-binding domain of p150^{glued}.

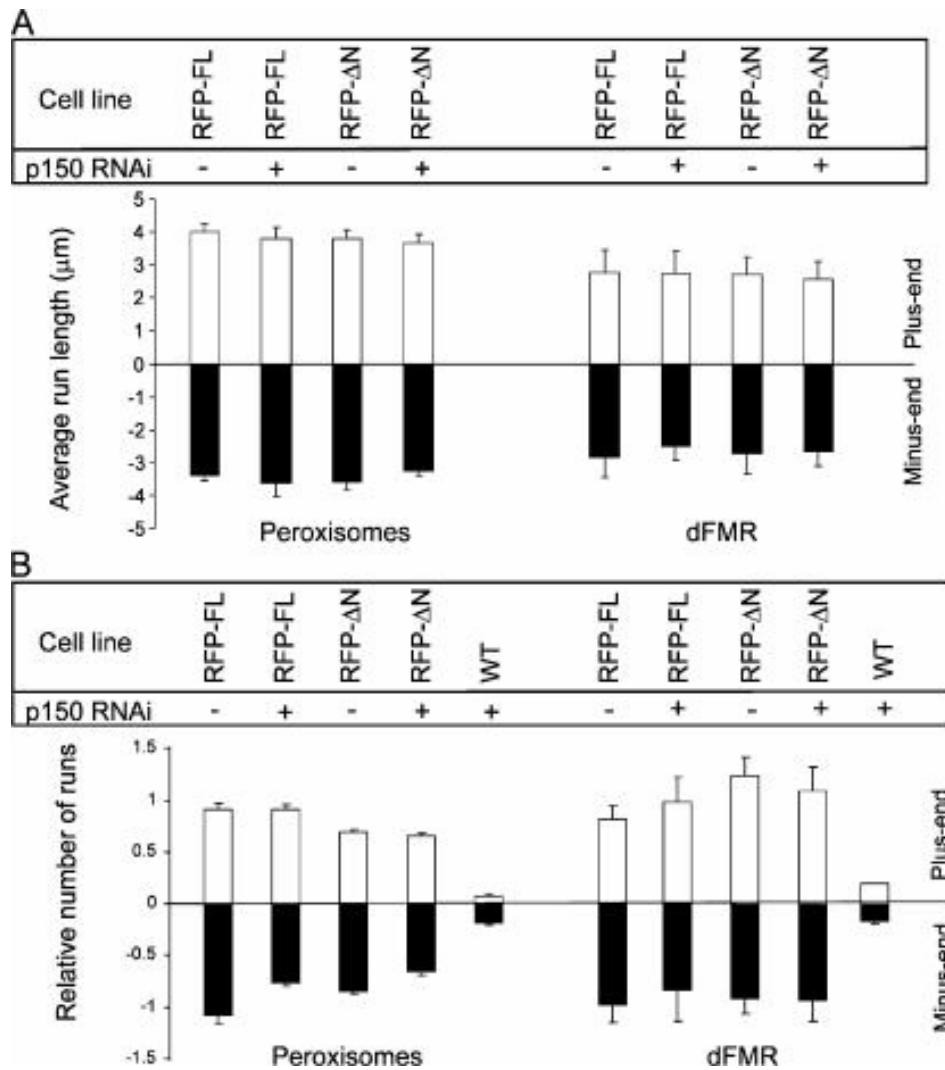


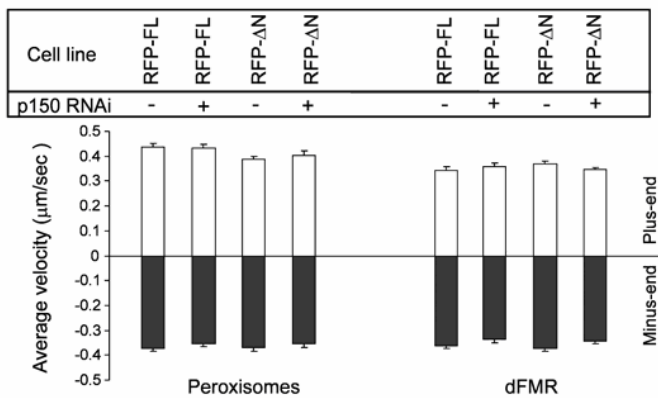
Figure 3.6. Deletion of the microtubule-binding domain of p150^{glued} has no effect on average run length (A) or relative number of runs (B) of both peroxisomes and dFMRP particles. Note that the relative number of runs in cells having no p150^{glued} protein dropped significantly, more than five-fold compared to the cells expressing mRFP-p150^{glued} or mRFP-ΔN-p150^{glued}. The average run length is calculated from the trajectory length of moving particle in the process without stopping or changing directions. Total number of particles analyzed for each treatment group in this experiment was 83, 147, 256, 268, and 113 for peroxisomes and 172, 142, 170, 337 and 111 for dFMR (numbers correspond to bars on the chart, from left to right).

In order to exclude the possibility that the results are limited in two particular cargoes, we examined the effect that removal of the microtubule-binding domain of p150^{glued} has on movement of other cargo; endosomes and lysosomes. Endosomes were labeled by incubating cells with Texas Red-conjugated dextran and lysosomes were labeled with LysoTracker. Movements of lysosomes and endosomes were not affected by truncation of the microtubule-binding domain (Fig 3.7B).

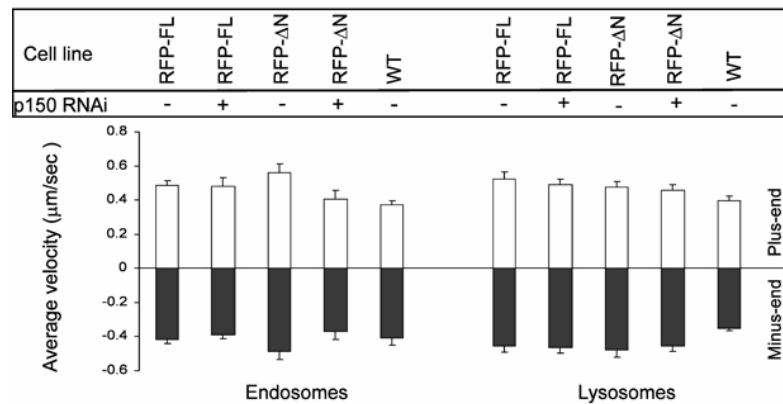
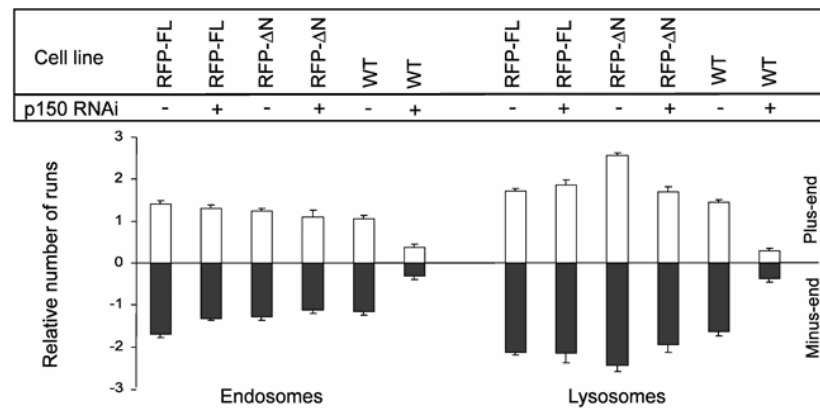
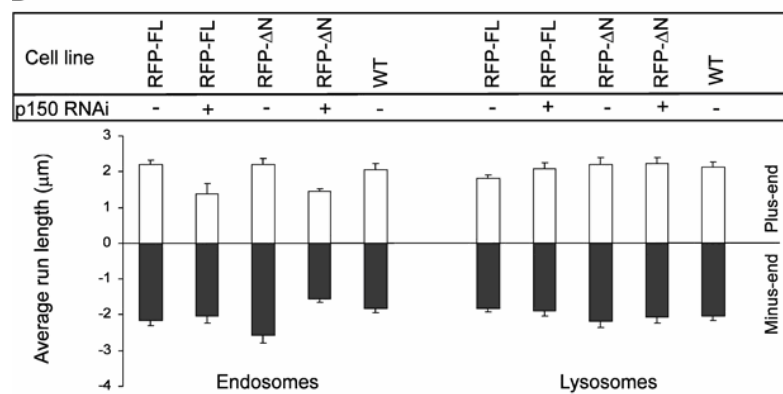
This study also examined the movement of peroxisomes in the absence of Cytochalasin D where actin filaments are intact. Δ N-p150^{glued} in this condition supports peroxisome transport identically to the wild type, which suggests that the absence of actin filaments induced by cytochalasin-D does not facilitate Δ N-p150^{glued}-mediated organelle transport.

This study also examined the steady-state distribution of peroxisomes, lysosomes, and endosomes in cells expressing wild type p150^{glued}, EGFP-p150^{glued}, or EGFP- Δ N-p150^{glued} (Fig 3.7C). Again cells were not treated with cytochalasin D. Truncation of the microtubule-binding domain did not affect organelle distribution, which suggests that Δ N-p150^{glued} mediates proper dynactin function as wild type in the presence of actin filaments. These results demonstrate that the microtubule-binding domain of p150^{glued} is not important for the movement of at least four types of cargo along microtubules in S2 cells.

A



B



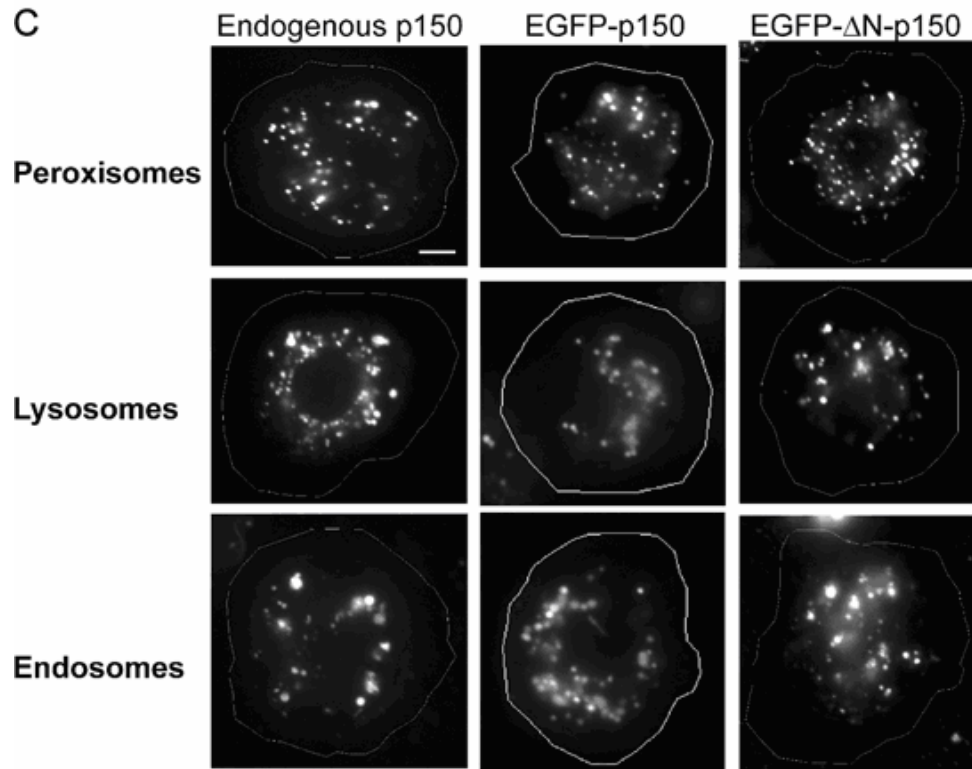


Figure 3.7. (A) Deletion of the microtubule-binding domain of p150^{glued} has no effect on average velocity of peroxisome or dFMRP particle.

(B) Deletion of the microtubule-binding domain of p150^{glued} has no effect on average run length (B1), relative number of runs (B2), or average velocity (B3) of both endosomes and lysosomes.

Note that replacement of the wild-type p150^{glued} with GFP-tagged full-length or truncated versions has no effect on motility, but there is a dramatic decrease in motility in the absence of p150^{glued}.

(C) The steady-state distribution of peroxisomes, lysosomes, and endosomes in S2 cells expressing wild type p150^{glued}, EGFP-p150^{glued}, or EGFP-ΔN-p150^{glued}.

Unlike cells used for motility analysis, cells in this experiment were not treated with cytochalasin

D. Truncation of the microtubule-binding domain did not affect organelle distribution. The outline of each cell is marked as lines. Scale bar, 10 μm.

3.3.6 Dynactin binding to microtubules suppresses the generation of multipolar spindles and free microtubule-organizing centers.

Drosophila cytoplasmic dynein and dynactin play critical roles during cell division that include spindle assembly and elongation, anaphase chromosome movements, and removal of spindle checkpoint components from attached kinetochores (Buffin et al., 2005; Morales-Mulia and Scholey, 2005; Robinson et al., 1999; Sharp et al., 2000a; Sharp et al., 2000b; Wojcik et al., 2001). To examine the mitotic contribution of the microtubule-binding domain of p150^{glued}, S2 cells expressing EGFP-p150^{glued} or EGFP-ΔN-p150^{glued} were treated with either control or dsRNA from the 3'-UTR of p150^{glued} and immunostained for both microtubules and the mitosis-specific phosphorylated histone H3.

Depletion of endogenous p150^{glued} in cells expressing EGFP-ΔN-p150^{glued} elevated the mitotic index 3-fold and increased the frequency of prometaphase-stage figures as compared to a control RNAi treated cells. A similar prometaphase-like arrest was also described for cultured mammalian cells overexpressing the dynactin inhibitor p50/dynamitin (Echeverri et al., 1996).

Unexpectedly, a significant increase was observed in multipolar spindles in cells expressing EGFP-ΔN-p150^{glued} (Fig 3.8), a phenotype not previously described for dynactin inhibition. Multipolar spindle formation is attributed to the failure to properly coalesce microtubule-organizing centers (MTOCs) during prometaphase, a mechanism that may depend upon a p150^{glued}-microtubule interaction. A previous study found that 39% of untreated prophase S2 cells contain four or more gamma tubulin-staining MTOCs, and live imaging of S2 cells expressing GFP-tubulin revealed a clustering and fusion mechanism that eliminates extra MTOCs following nuclear envelope breakdown (Goshima and Vale, 2003). Consequently, failure to cluster and fuse extra MTOCs resulted in multipolar spindle formation.

Furthermore, Quintyne et al. (Quintyne et al., 2005) identified dynein as a critical component of a centrosome clustering mechanism present in human tissue culture cells that when mislocalized in certain tumor cells results in multipolar spindle formation. Consistent with this hypothesis, we found that cells expressing EGFP- Δ N-p150^{glued} exhibited a dramatic increase in the number of free MTOCs that were surrounded but did not incorporate into mitotic spindles (Fig 3.8). Thus, the microtubule-binding domain of p150^{glued} is required to suppress multipolar spindle formation by coalescing extra MTOCs frequently present in many early mitotic S2 cells.

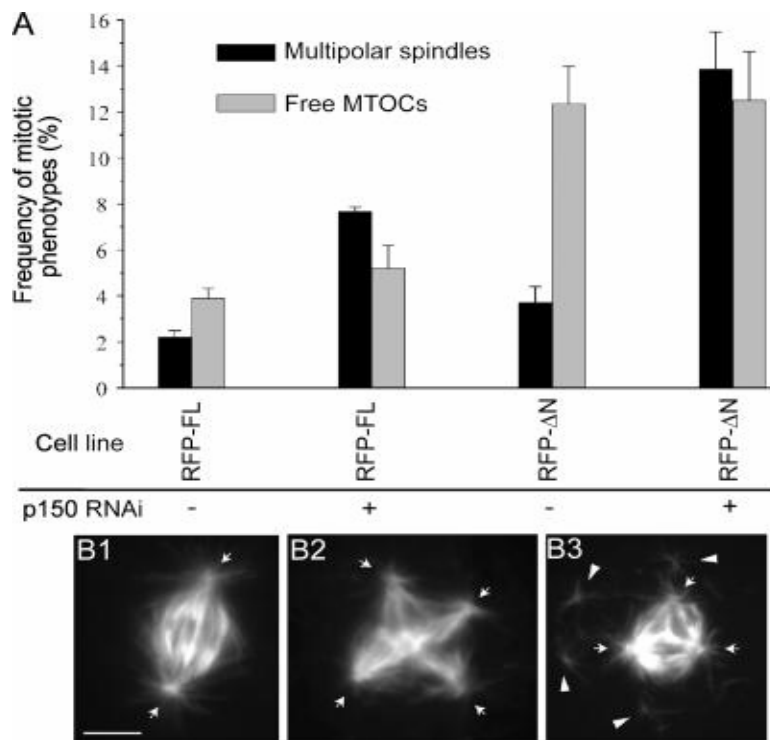


Figure 3.8. Replacement of p150^{glued} with EGFP- Δ N-p150^{glued} results in the accumulation of multipolar spindles and non-spindle associated (free) MTOCs.

(A) Percentage of multipolar spindles and free MTOCs present in average 200 mitotic cells per RNAi. **(B)** Mitotic cells stained for microtubules. (B1) Normal metaphase in the control cell, (B2) multipolar spindles and (B3) free MTOC in cells expressing EGFP- Δ N-p150^{glued}. Free MTOCs are labeled with arrowheads and spindle poles are with arrows. Scale bar, 5 μ m.

3.4 DISCUSSION

Adaptors between motors and cargo are a diverse group of cellular proteins, but the most universal of them is the dynactin complex. An unusual property of this complex is its ability to bind microtubules independently of motor proteins. Here, the functional significance of microtubule binding by dynactin was addressed by replacing endogenous p150^{glued} with a p150^{glued} mutant that is not able to bind microtubules (Δ N-p150^{glued}).

Stable cell lines expressing mRFP-tagged p150^{glued} or Δ N-p150^{glued} were selected and depleted with endogenous p150^{glued} by RNAi. This approach allowed examination of the function of microtubule-binding domain of p150^{glued} to cargo transport as well as to the organization of spindle microtubule arrays. This study demonstrated that movement of two types of cargo, membranous organelles (peroxisomes, endosomes, and lysosomes) and mRNP complexes (dFMRP particles) is absolutely dependent on the dynactin complex, but that Δ N-p150^{glued} lacking the ability to bind microtubules was fully functional in supporting microtubule-dependent transport *in vivo*. All the measurements were done in the cells treated with cytochalasin D to eliminate actin-based motility.

We observed a profound effect resulting from the truncation of microtubule-binding domain on spindle structure, including the generation of multipolar spindles and free microtubule-organizing centers. Although dynactin plays an important role in organizing the interphase radial microtubule arrays at the centrosome in mammalian cultured cells (Askham et al., 2002; Quintyne et al., 1999; Quintyne and Schroer, 2002), no significant changes were observed in the pattern of interphase microtubules in S2 cells expressing Δ N-p150^{glued}. A possible explanation for this is the fact that S2 cells lack functional centrosomes capable of nucleating and organizing microtubules during interphase. Instead, microtubules nucleate at

random in the cytoplasm and do not form a focused radial array (Rogers, GC, Rusan, NM and Rogers, SL; manuscript in preparation).

It is worth noting that one of the p150^{glued} isoforms in mammalian brains is an alternatively spliced version called p135, which naturally lacks the microtubule-binding motif (Tokito et al., 1996). As neurons are terminally differentiated cells that do not divide, they may not need dynactin activity to facilitate spindle microtubule organization. In addition, the results presented here suggest that this alternatively spliced isoform, p135, is as effective as the full-length p150^{glued} in supporting neuronal transport.

Three possible functions have been proposed for the microtubule-binding domain of p150^{glued}. First, King et al. (King and Schroer, 2000) demonstrated that the dynactin complex increases the processive movement of beads coated with cytoplasmic dynein *in vitro*. This idea is further supported by two recent papers (Culver-Hanlon et al., 2006; Kobayashi et al., 2006) showing that p150^{glued} is capable of one-dimensional diffusion along microtubules and thus maintains contact with microtubules. Therefore, enhanced processivity *in vitro* can be achieved by the p150^{glued}-microtubule interaction. In contrast, the results shown here indicate that the effect of microtubule binding on motor processivity is sufficiently minor.

There are several potential explanations of an apparent discrepancy between our results and the previous *in vitro* studies (King et al., 2003; King and Schroer, 2000). First, it is not known if four types of cargo studied here are transported by single or multiple dynein motors. If cargo were transported by more than one dynein, then dynactin would not contribute to the processivity significantly. Furthermore, several redundant mechanisms may be involved in the regulation of dynein processivity in cells and thus the effects of the truncation of the microtubule-binding domain might not be immediately obvious if other putative mechanism(s)

is/are in action. Second, previous studies were performed *in vitro*; not with the native dynein-dynactin complex, but with two protein complexes bound separately to the surface of carboxylated beads. It is unclear if all the properties of dynein-dynactin complex on the surface of organelles can be faithfully recapitulated by binding of purified proteins to highly charged beads. Finally, *in vitro* assays were performed under no-load conditions, and it is possible that the load applied to organelles in the cytoplasm affects processivity of transport.

In agreement with our finding, a recent study using a purified dynein-dynactin complex from *S. cerevisiae* and a single molecule TIRF microscope, demonstrated that dynactin increased the processivity of dynein by approximately threefold, and that this function required a longer p150^{glued} fragment including both microtubule binding domain and coiled-coil stalk, and was not supported by the microtubule binding domain alone (Kardon et al., ASCB poster 2007).

The second potential role of the microtubule-binding domain of p150^{glued} was proposed by Vaughan et al. (Vaughan, 2005a; Vaughan et al., 2002). These authors suggested that p150^{glued} tethering to the plus-ends of growing microtubules facilitates the loading of retrograde cargo on plus-ends of microtubules. This function would require the interaction of dynactin with microtubules. The truncated form of p150^{glued}, ΔN-p150^{glued}, should not function to load cargo onto microtubules. However, in the case of the two types of cargo examined in this study, such a ‘search and capture’ mechanism is not a major contributor towards retrograde transport by dynein because the removal of microtubule binding from dynactin did not affect cargo transport.

In agreement with these results, Watson and Stephens showed that depletion of either EB1 or CLIP-170 resulted in a loss of p150^{glued} from microtubule plus-ends, but did not affect trafficking of membrane organelles (Watson and Stephens, 2006). It is likely that a combination of microtubule dynamics and Brownian motion of cargo is sufficient to make initial contact and

thus load cargo onto microtubules. Thus, microtubule plus-end targeting of p150^{glued} is not required for cargo loading. However, it would be interesting to examine the effect of Δ N-p150^{glued} on cargo transport in the cellular regions containing single microtubules instead of cytochalasin D-induced microtubule bundles, in order to determine the kinetic advantages of a ‘search and capture’.

Finally, we suggest that p150^{glued} functions through its microtubule binding domain to pull and focus spindle microtubules, and to prevent formation of multipolar spindle or free microtubule organizing centers. We observed a dramatic defect of truncation of the microtubule-binding domain on mitotic spindle structure stressing the essential role of N-terminal microtubule binding domain of dynactin on microtubule organization. This supports the role of centrosomal dynactin on microtubule “anchoring” function proposed by Quintyne et al. (Quintyne et al., 1999).

Dynactin is also required for microtubule anchoring at cell cortex or at kinetochores. A recent study in budding yeast has provided evidence that the microtubule-binding domain in p150^{glued} has a role in transferring dynein from microtubule ends to binding sites at the cell cortex prior to motor activation, thus facilitating proper spindle organization (Moore JK et al, ASCB poster 2007).

Taken together, the data demonstrates that the microtubule-binding domain of p150^{glued} has a significant role in spindle microtubule organization, but is not required for long-range movement of cargoes along microtubules by motor proteins *in vivo*.

CHAPTER 4: MICROTUBULE MOVEMENT *IN VIVO* BY KINESIN-1

4.1 SUMMARY

We have focused on how motor proteins transport cargo along microtubules with the assumption that microtubule tracks are not significantly motile. However, there are several examples of interphase microtubule transport in neurons and epithelial cells. This microtubule movement may affect cargo transport. What is the source of force required to generate microtubule movements? The answer to this question is important to understand how cargo transport is affected by moving tracks and thus to speculate about the possible role of microtubule movement in other cellular processes.

Imaging of fluorescent microtubules in S2 cells demonstrated that microtubules are highly dynamic and undergo large-scale displacement. We generated a cell line expressing tubulin tagged with a photoconvertible protein Dendra2, which allowed us to mark microtubules and trace their movement over time.

To examine whether motors are required for microtubule transport, cells were treated with RNAi against different motors. Microtubule transport was significantly inhibited by knock-down of kinesin-1, while knock-down of other kinesins, cytoplasmic dynein, or dynactin complex did not affect microtubule transport.

How does kinesin-1 transport microtubules? We propose that the second microtubule binding domain at the C-terminus of kinesins-1 cross-links two microtubules and slides as kinesin-14 family (ncd) does. Surprisingly, a mutant kinesin at the second microtubule binding domain did not affect peroxisome transport, but it inhibited significantly microtubule movements.

Thus, we conclude that kinesin-1 transports microtubules and C-terminal microtubule-binding domain is required for this function.

4.2 RESULTS

4.2.1 Microtubules are highly motile in S2 cells.

During the observation of fluorescent microtubules in S2 cells, we found that microtubules in the cytoplasm were highly motile and displaying sliding and looping (Fig 4.1). A correlation between two peroxisomes moving along the same microtubule suggests that the microtubule track itself could move and possibly affect organelle transport (Kulic I at Harvard University). Microtubule bundles in processes induced by cytochalasin D are less dynamic compared to microtubules in cell body. Potential sources of this movement could be from the process of microtubule polymerization or depolymerization (Rodionov and Borisy, 1997), or from motor proteins generating force for microtubule transport (Baas et al., 2006; Oladipo et al., 2007; Straube et al., 2006).

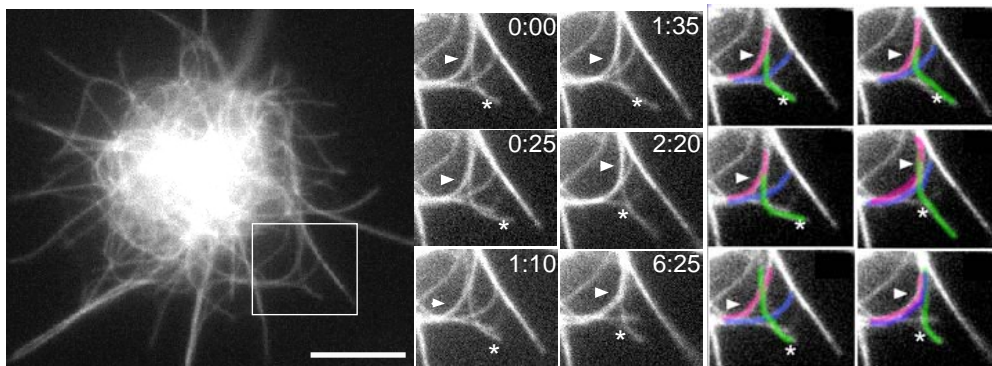


Figure 4.1. The microtubules in the S2 cell cytoplasm are highly motile and keep sliding and looping. A fluorescent image of a S2 cell expressing mCherry-tagged tubulin proteins (left). Right frames correspond to the boxed area in the left image (numbers represent min: sec). An arrow, a star and colors (right) were inserted to indicate moving microtubules. Scale bar 10 μ m.

4.2.2 The suppression of microtubule dynamics (the process of polymerization or depolymerization) does not affect microtubule movement.

In order to investigate whether the process of polymerization or depolymerization of microtubules drives microtubule movement, we examined microtubule movement after suppressing microtubule dynamics by treating cells with Taxol. Since long-term treatment of cells with Taxol changes microtubule distribution and length significantly, cells were treated with a low dosage of Taxol (5 μ M) for a brief period of time (10-30 min). No significant cell damage occurred during this time period. This treatment was sufficient to block localization of GFP-tagged EB1 protein to tips of microtubules as shown in [Figure 4.2](#).

EB1 binds to plus-ends of growing microtubules during polymerization (Mimori-Kiyosue et al., 2000) ([Fig 4.2A](#)). The absence of GFP-EB1 “comet-tail” ([Fig 4.2B](#)) after Taxol treatment indicates the suppression of microtubule dynamics. Surprisingly, the motion of microtubules was not changed by Taxol treatment, leading to the conclusion that the force generating microtubule movement is not from the process of microtubule polymerization or depolymerization.

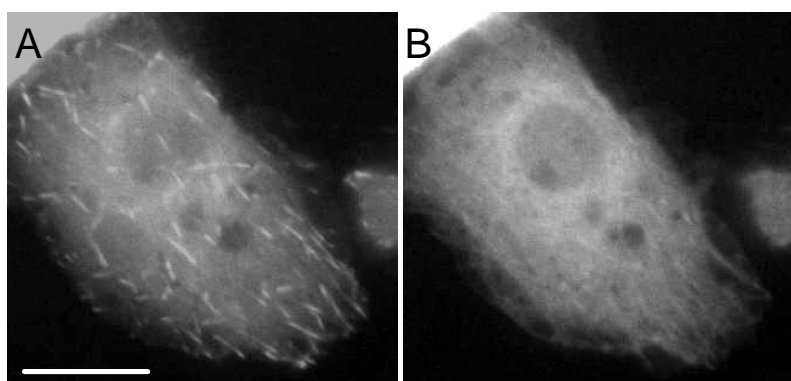


Figure 4.2. The treatment of Taxol inhibits the localization of GFP-tagged EB1 protein to tips of microtubules. Cells were treated with 5 μ M of Taxol for 10-30 min. No significant cell damage occurred for this time period. Panel (A) shows a cell before Taxol treatment and panel (B) shows the same cell after Taxol treatment. Scale bar, 10 μ m.

4.2.3 Generation of stable cells expressing photoconvertible tubulin.

Analysis of microtubule movement could be greatly facilitated by marking microtubules. We generated stable S2 cells which express photoconvertible protein Dendra-2 (Gurskaya et al., 2006) fused to a *Drosophila* α -tubulin under control of the metallothionein promoter. Cells were treated with CuSO₄ for the induction of α -tubulin protein and incubated for 12-24 hrs until tubulin monomers were incorporated into microtubules. Before photoconversion, Dendra-2 has a characteristic emission peak of 505 nm (green), but after exposing it to a 405 nm wavelength of intense light (Mercury or laser) it shifts its peak to 575 nm (red). A slit was inserted in the light path to photoconvert Dendra-2 proteins in a small region (Fig. 4.3).

Cells were treated with Cytochalasin D to inhibit retrograde actin flows at the cell periphery; these actin flows may affect microtubule movement. Fluorescent tubulin monomers are rapidly incorporated in polymerizing microtubule ends and it is difficult to track photoconverted microtubule segments in such high background of fluorescent tubulin. Therefore, a soluble pool of tubulin was depleted by treating cells with microtubule-stabilizing drug (Taxol).

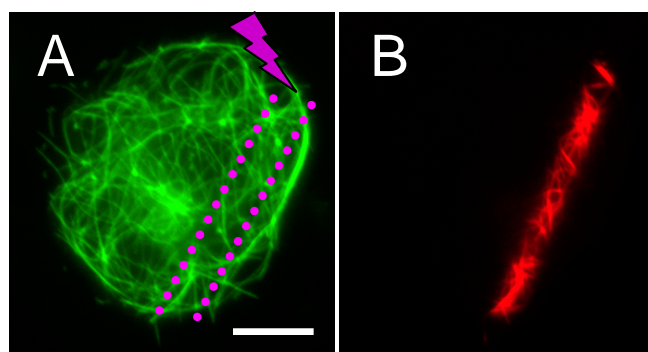


Figure 4.3. Photoconversion of Dendra2-tagged tubulin in a S2 cell.

The fluorescent color of microtubules changes from green to red after 405 nm exposure. Panel A (before photoactivation), shows a standard microtubule pattern in interphase S2 cells. Panel B shows a photoconverted microtubule pattern in a small region. Scale bar, 10 μ m.

We quantified the microtubule movement by counting the number of microtubules translocated from a photoactivated zone (slit area) to the rest of cell area for 5 min after photoconversion (Fig 4.4). The average number of motile microtubules in wild type S2 cells is 36 ± 4 (mean \pm SD) per cell. The speeds of motile microtubules were measured by tracking microtubule tips manually using metamorph software. Figure 4.5 shows a speed distribution of motile microtubules from the cell shown in Figure 4.4. The average speed of each microtubule above threshold speed ($0.15 \mu\text{m}/\text{sec}$) were in the range of $0.2\sim 0.4 \mu\text{m}/\text{sec}$, which is the speed of microtubule-dependent motors. In most cases, microtubules were motile $\sim 10\%$ of the time of recording (5 min) and remained stationary for the rest of time ($\sim 90\%$).

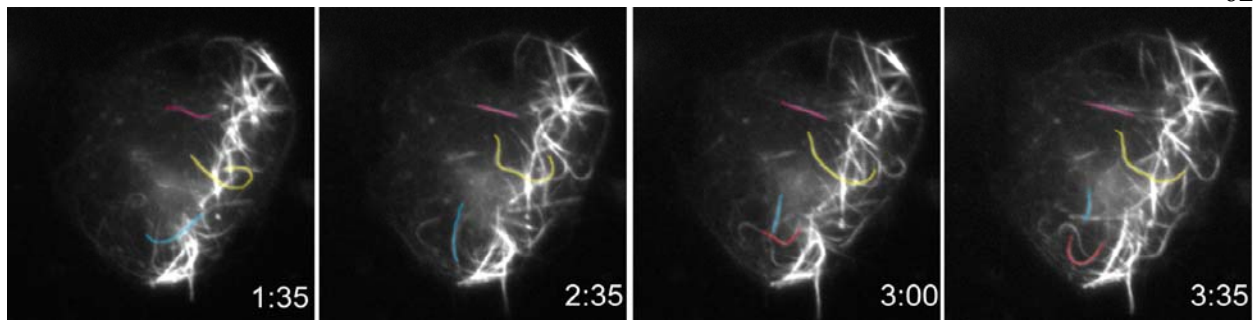


Figure 4.4. Fluorescent images of a S2 cell expressing Dendra2-tubulin after photoconversion (numbers represent min: sec). Subsets of microtubule segments were presented in colors. This time-lapse images show again that microtubules in S2 cells are highly motile.

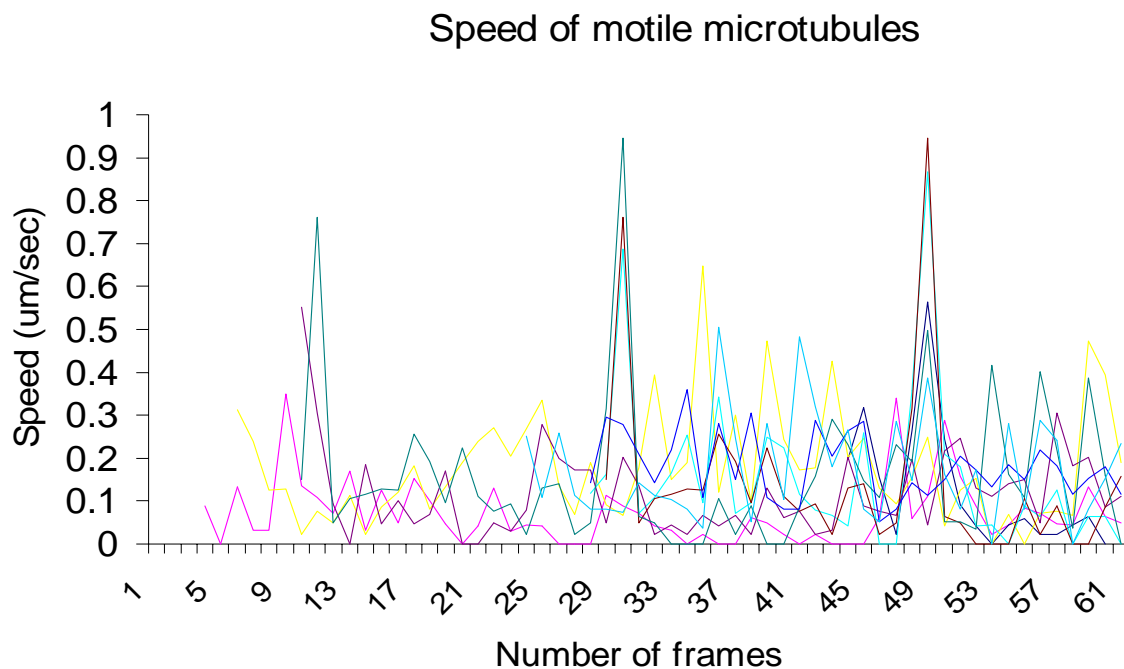


Figure 4.5. A speed distribution of motile microtubules. Speed profiles of nine individual microtubules are shown in different colors from 61 frames of a time-lapse movie for 5 min.

4.2.4 Kinesin-1 transports microtubules in S2 cells.

In order to identify motor proteins required for microtubule movement, RNAi-mediated knock-down of several kinesins, cytoplasmic dynein or subunits of the dynactin complex, was performed. [Figure 4.6A](#) shows the average number of moving microtubules after photoconversion in cells treated with dsRNA against different motors. The average numbers were represented as percentage compared to control (wild type) cells. Western blots against several motors were shown in [Figure 4.6B](#).

Several motors are known to be involved in the movement of spindle microtubules during mitosis. These motors include *Drosophila* Klp61F (kinesin-5 family) and C-terminal kinesin, Ncd (kinesin-14 family). Surprisingly, microtubule movement was significantly inhibited by knock-down of kinesin heavy chain (KHC) and kinesin light chain (KLC), while knock-down of other mitotic kinesins and kinesin-2 did not affect microtubule movement. Similarly, knock-down of either dynein heavy chain (DHC) or dynactin subunit, p50-dynamitin did not affect microtubule movement. Previous study in our lab showed that the depletion of dynein and dynactin complex completely blocked transport of organelles and mRNA particles (Kim et al., 2007; Ling et al., 2004). This result excludes the possibility that microtubule movement is from the reactive force generated by cargo moving forward along the microtubules, and leads to the conclusion that kinesin-1 is required for movement of interphase microtubules in S2 cells.

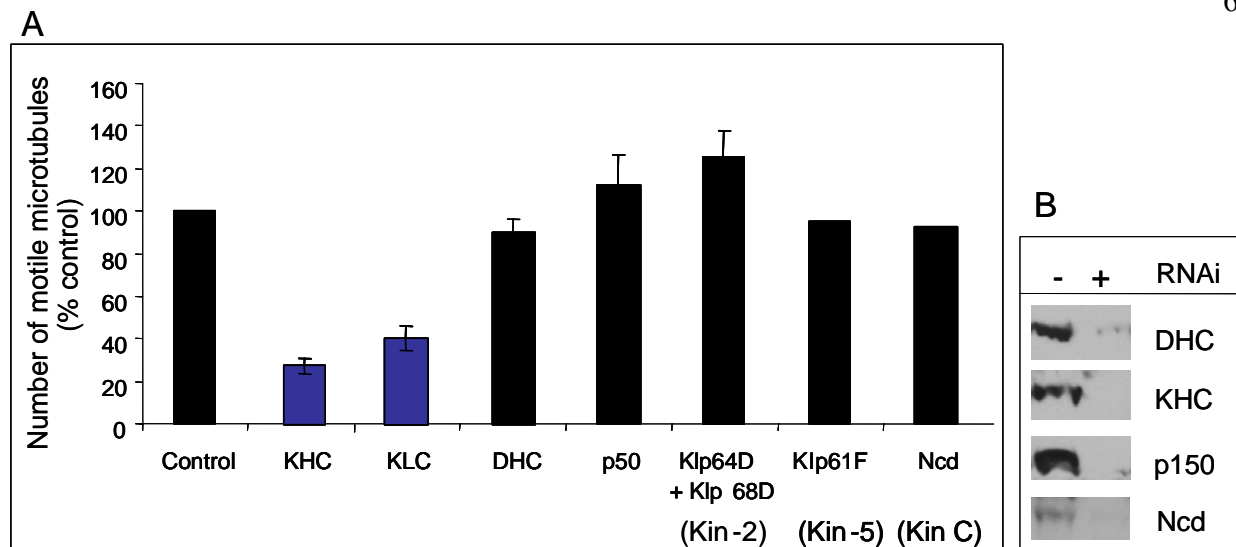


Figure 4.6. (A) A diagram showing the relative number of motile microtubules after knock-down of several motor or adaptor proteins. The average numbers of moving microtubules were represented as percentage compared to the control (wild type) cells. **(B) Western blots of S2 cell extracts from cells before and after RNAi mediated knock-down**

4.2.5 Mechanism of kinesin-1-driven microtubule movement.

How does kinesin-1 move microtubules in the cytoplasm? Expression of a human kinesin-1 tail fragment in CV-1 monkey kidney epithelial cells demonstrated that the C-terminal 196 amino acids of human kinesin heavy chain (KHC) was localized to microtubules *in vivo* (Navone et al., 1992), which suggests the presence of a second microtubule-binding domain in KHC. More recently, Hackney and Stock (Hackney and Stock, 2000) mapped this second binding domain to 883-937 amino acids residues in *Drosophila* KHC (Fig 4.7A) and further showed that this binding is independent of the presence of ATP. We propose that kinesin-1 cross-links two microtubules through its C-terminal tail domain and slides microtubules against each other (Fig 4.7B).

We created a mutant KHC where four positively-charged residues in the microtubule-binding region were replaced with alanine residues (K925A R929A H932A R936A, Mut-A) (Fig 4.7A) to inhibit its electrostatic interaction with negatively charged microtubules. Electrostatic tethering interaction is known to play a major role on stabilizing interaction between kinesin-1 and microtubules (Thorn et al., 2000). To replace wild-type kinesin-1 with a mutant form, we transfected S2 cells with a plasmid that encodes full-length wild-type or mutant heavy chains under the control of metallothionein promoter. Stable cells were selected by hygromycin. These cells were treated with ds RNA corresponding to the 5'-untranslated region (UTR) of KHC mRNA to deplete the endogenous protein. To induce the expression of either wild-type or mutant protein, cells were incubated for 12-16 hrs with CuSO₄. Western blotting analysis with an antibody that recognize the conserved motor domain of kinesin-1 demonstrated that, after protein induction, the stable cell line expressed the new protein with the same molecular weight as the wild type KHC (Fig 4.7C).

Induced cells were examined for their ability to move peroxisomes, whose motility is known to be driven by kinesin-1 (Kim et al., 2007; Kural et al., 2005). As shown in Figure 4.8A, the mutation of four charged residues in positions 925-936 of KHC did not affect the ability of kinesin-1 to transport peroxisomes. This was expected, as peroxisomes are known to bind to KHC through the kinesin light chain (KLC) for its transport (Ling et al., 2004). However, the number of moving microtubules decreased significantly in cells expressing the mutant KHC (Mut-A). The decreased level was similar to the level in cells where KHC was depleted completely by dsRNA against KHC coding sequence (gene-specific RNA; see white bars in Fig 4.8B). Figure 4.9 shows a representative cell which expresses mutant KHC and is depleted endogenous wild type kinesin. There were few motile microtubules found for 5 min of recording

time after photoactivation. We thus conclude that kinesin-1 transports microtubules and its C-terminal microtubule binding domain is required for this function.

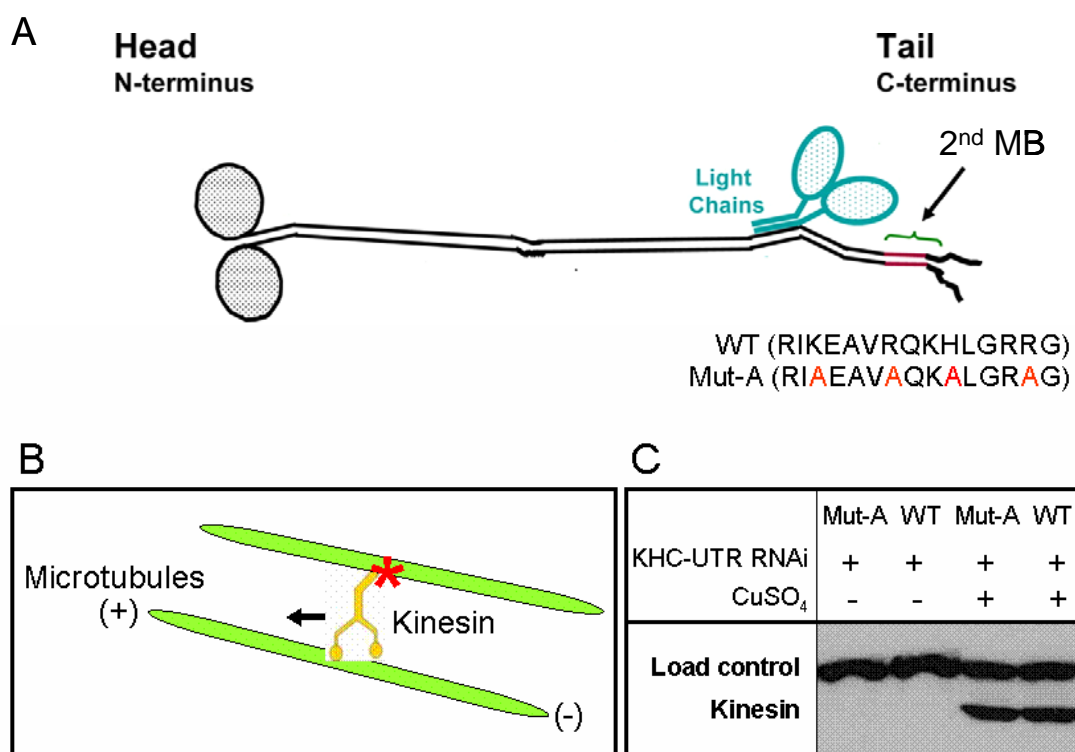


Figure 4.7. (A) Design of a kinesin mutant where four positively-charged residues in the C-terminal microtubule-binding region were replaced with alanine residues (K925A R929A H932A R936A, Mut-A) (B) The mechanism of microtubule transport by kinesin-1 (C) The examination of kinesin expression levels by Western blot analysis. The endogenous wild type kinesin was suppressed by RNAi of the UTR region of KHC, and the exogenous mutant kinesin or wild type kinesin under an inducible promoter, was induced by CuSO₄ incubation.

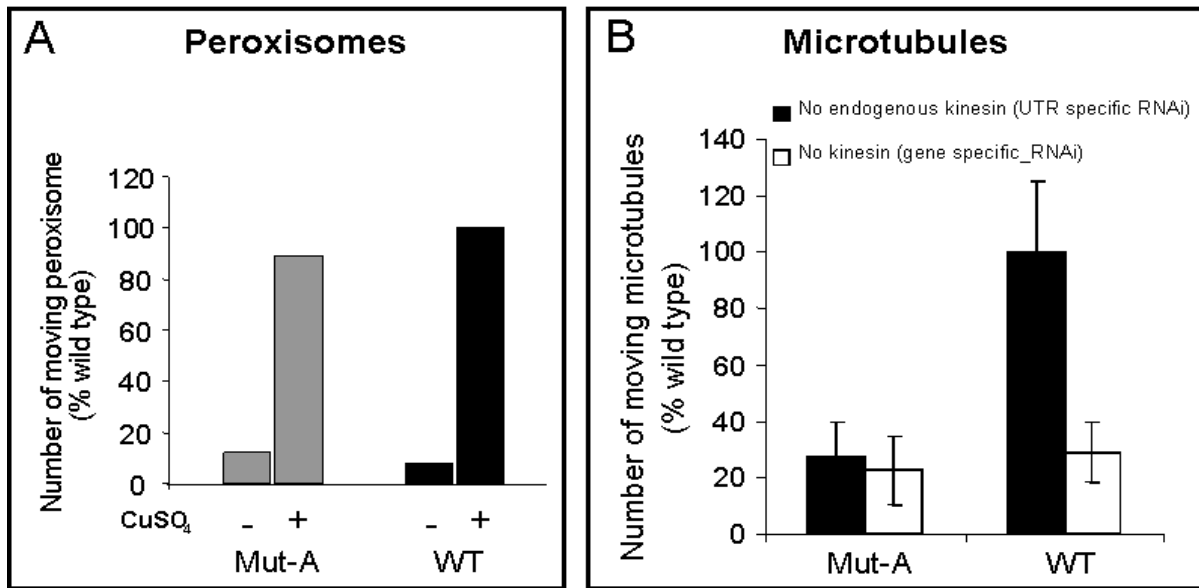


Figure 4.8. Effect of mutant kinesin on organelle and microtubule motility.

(A) A diagram showing the relative number of moving peroxisomes in cells expressing either wild type or mutant kinesin. No significant changes on peroxisome transport by mutant kinesin.

(B) A diagram showing the relative number of motile microtubules in cells treated either kinesin -UTR specific RNA or -gene specific RNA. Note that the inhibitory effect by mutant kinesin on microtubule movements was as severe as the effect from complete knock-down of kinesin.

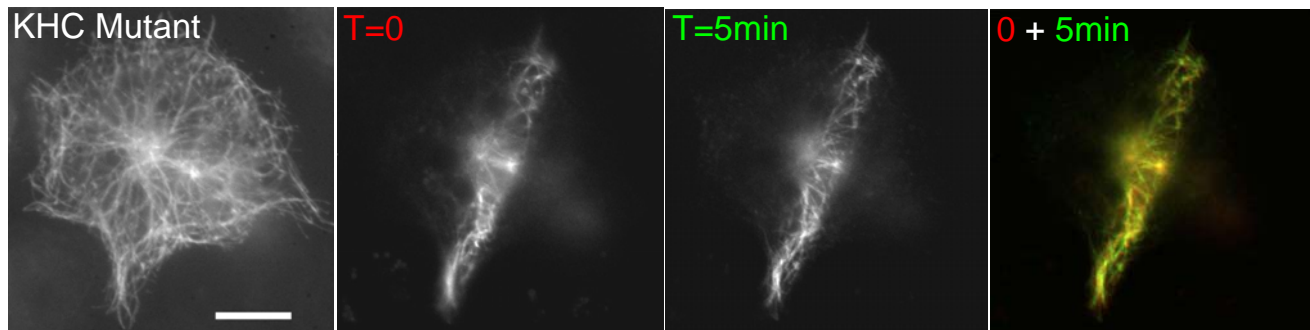


Figure 4.9. A time-lapse movie showing the effect of mutant kinesin on microtubule movements

A fluorescent image before activation (FITC filter) and florescent images after activation (Texas red filter) of the same cell. False-colored image (far right) merges images that span a time interval of 5 min (T=0 in red; T=5 min in green). Scale bar, 10 μ m.

4.3 DISCUSSION

This study has shown that microtubules are dynamic structures which might affect many cellular processes, including organelle transport, mitotic spindle organization, and polarized cell growth. We showed that kinesin-1 is required for microtubule movement by forming cross-bridges between adjacent microtubules through the C-terminal microtubule binding domain in its heavy chain. We suggest that KHC hold one microtubule through C-terminal binding domain and walk toward the plus end of the other microtubule at the same time, thus resulting sliding of microtubules.

We focused mainly on the function of KHC on microtubule transport. However, our results showed that the depletion of KLC also inhibited microtubule transport as severely as KHC. We speculate that KLC may interact with other regulatory proteins which have microtubule binding activity and possibly cross-link microtubules, but such proteins have not been identified as yet.

Hackney and Stock (2000) assigned an *in vitro* microtubule binding domain to a stretch of 55 amino acids between the organelle binding region and the ATP regulation site, which is highly conserved from fungus to human. *In vivo* imaging of microtubule organization in the fungus *Ustilago maydis* (Straube et al., 2006) has shown that kinesin-1 mediates microtubule-microtubule interactions through its conserved C-terminal tail domain. Moreover, the rigor-mutant in the motor head suppresses microtubule motility but promotes strong microtubule bundling, which strongly supports the line of thought that kinesin-1 forms cross-bridges between microtubules and generates force (or tension). This study showed that interaction between KHC and microtubules are compromised by replacing (+) charged amino acids with alanines at this conserved C-terminal microtubule binding domain.

This study has described highly motile microtubule structures in S2 cells. Such movements have not been observed in other tissue cultured cells where microtubules did not show any dramatic movement (Oladipo et al., 2007). One difference in our system is that cells were treated with Cytochalasin D, while other studies examined cells with intact actin filaments. The actin filament network might itself change the behavior of microtubules. The majority of microtubules in *Xenopus* melanophores also do not demonstrate significant microtubule movements compared to microtubules in S2 cells. Interestingly, microtubule motility was enhanced 5-6 fold after depletion of actin filaments by Cytochalasin D (Jolly A in the lab of Dr. Gelfand, unpublished data).

Intact actin filaments might inhibit kinesin-based microtubule transport by acting as a physical barrier; either by themselves or through linker proteins that interact with both actin and microtubules (Kerkhoff, 2006; Rosales-Nieves et al., 2006). Several regulatory proteins (such as ACF7, an integrator of two cytoskeletal systems) have been shown to control microtubule dynamics and reinforce links between microtubules and actin filaments (Kodama et al., 2003). Therefore, one way of regulating microtubule movement would be to change the local concentration of actin filaments or modulate the activity of binding proteins. Actin filaments could function as an additional regulatory factor that restricts microtubule movement and this restriction can be released by an actin depolymerizing drug. This implies that the balance between two cytoskeletal systems is important for kinesin-dependent cellular processes, which has been shown in cytoplasmic streaming in *Drosophila* oocytes (Serbus et al., 2005).

One immediate question that should be addressed is whether the microtubule transport mechanism mediated by kinesin-1 is also found in other cell types. The methodology of this study, such as photoconversion of tubulin and RNAi of kinesin-1, can be used to answer this.

CHAPTER 5: CONCLUSION

The goal of this research was to contribute to our understanding of the molecular mechanisms that regulate bidirectional, microtubule-based organelle transport *in vivo*. The research presented in this dissertation accomplished this goal by analyzing *in vivo* step-sizes of kinesin-1 and dynein motors and examining organelle movement after depletion of motors (discussed in Chapter 2), exploring the role of microtubule binding by dynactin on organelle transport (discussed in Chapter 3), and studying mechanisms controlling microtubule movement (discussed in Chapter 4).

The results presented in Chapter 2 demonstrate the stepping behaviors of a peroxisome carried by kinesin-1 and dynein *in vivo*. The goal of this study was to address how kinesin and dynein work together to transport the same cargo *in vivo*. Studies in live cells had not been performed previously. The data presented here describe a novel *in vivo* approach that may be applied in other systems. We showed that both kinesin and dynein motors conserved their stepping behaviors as 8 nm steps on the surface of actual cargo *in vivo*.

We showed that impairment of transport in one direction by knock-down of either kinesin-1 or dynein did not improve transport in the other direction, but abolished bidirectional motility completely. In addition, we did not observe hyper-aggregation or hyper-dispersion of peroxisomes after RNAi of either kinesin or dynein, but instead observed complete inhibition of bidirectional transport. These results suggest that kinesin-1 or dynein alone cannot support transport in either directions and that both motors are required for proper organelle transport and localization *in vivo*.

It is not known how the presence of one motor affects the other motor. The opposing motor may be required for the proper orientation of a motor for its full activity. In future studies, kinesin mutants with reduced in ATPase activity, and with the same microtubule binding and cargo interacting activities, could be examined to determine whether they support dynein-driven organelle transport and show a hyper-aggregation phenotype.

The results presented in Chapter 3 describe the role of microtubule binding by dynactin complex for microtubule-dependent organelle transport. The goal of this study was to determine whether microtubule binding by dynactin affects the motor's processivity or other motile properties *in vivo*. Interestingly, while movement of both membranous organelles and mRNP complexes require an intact dynactin complex, the substitution of full-length p150^{glued} with ΔN-p150^{glued} did not affect the processivity, run length, or velocity of transport.

However, the truncation of the microtubule-binding domain of p150^{glued} induced dramatic defects on mitotic spindle structure such as multipolar spindles and free microtubule-organizing centers. We suggest that p150^{glued} functions through its microtubule-binding domain to pull and focus spindle microtubules, and to prevent formation of multipolar spindle or free MTOCs.

We conclude that dynactin has important role in organelle transport but not through its microtubule binding domain. Since dynactin has diverse roles and its function by microtubule binding could be more complex than was originally thought. In the future, the S2 cell system used in our study could be used to determine which domain of p150^{glued} is important to enhance processivity and whether other subunits (or specific domains) of dynactin affect processivity.

The results of Chapter 4 describe microtubule transport in S2 cells and a novel role of kinesin-1 as a force-generator for microtubule movement. The goal of this study was to identify the molecular mechanism of microtubule movement and explain its possible role on organelle

transport. Three potential sources of the force were proposed for generating microtubule movement: (i) Microtubule polymerization or depolymerization, (ii) Reactive force generated by cargo moving forward along microtubules, (iii) Dedicated motor-driven mechanism. The first two possibilities were ruled out by suppressing microtubule dynamics by treating cells with Taxol and by knocking down several motor proteins responsible for organelle transport.

We demonstrated that kinesin-1 is required for microtubule movement and we proposed the mechanism by which kinesin-1 generates the force for microtubule movement: crosslinking two microtubules through C-terminal microtubule binding domain of kinesin-1. However, the role of microtubule movements on organelle transport is not known yet. Here, we showed that a mutant kinesin based on its C-terminal microtubule binding domain, supports organelle transport as same as wild type does. An analysis of organelle tracking at high temporal and spatial resolution (using FIONA for example) in the presence or absence of highly motile microtubules would help us understand any subtle relationship between organelle and microtubule movements. In addition, the potential role of actin filaments in restricting kinesin-mediated microtubule transport should be addressed in the near future.

The research presented in this dissertation has contributed to the overall understanding of the microtubule-based transport. We provided evidence of interdependence between kinesin-1 and dynein. We showed that the function of microtubule binding by dynactin is not required for transport, but has an important role in spindle microtubule organization. The results of kinesin-1-mediated microtubule movements provided new insights to the understanding of microtubule-dependent transport. Future work on the mechanisms controlling microtubule organization by other cytoskeletal systems and cross-talk between microtubules and actin filaments would contribute to the understanding of how different cytoskeleton systems work together.

CHAPTER 6: MATERIALS AND METHODS

6.1 Molecular cloning

The cDNA for *Drosophila* p150^{glued} (clone AY118377, Open Biosystems, Huntsville, AL) and Δ N-p150^{glued} construct encoded amino acids residue 201-1280 were amplified and subcloned into pAc5.1/V5-HisA vector (Invitrogen). EGFP or mRFP sequence was introduced at the N terminus of p150^{glued}. To make His₆-tagged p150^{glued}, sequence of p150^{glued} encoding residues 1-600 or 200-600 was subcloned into pET28 (a+) (Novagen/EMD Biosciences, San Diego, CA). The first coiled-coil domain (CC1, amino acid 232-583) of p150^{glued} or the full-length p50/dynamitin was fused to mRFP to create the dominant-negative constructs mRFP-CC1 and mRFP-p50 in pMT5.1/V5-HisA vector.

Drosophila alpha-tubulin gene was amplified and subcloned into pMT.A vector (Invitrogen). EGFP, mCherry or Dendra2 sequence was introduced at the N terminus of alpha-tubulin. To introduce point mutations in the C-terminal microtubule-binding region of KHC (Ala mutant; K925A R929A H932A R936A), overlapping PCR technique was used and its final construct was confirmed by sequencing. The C-terminal fragments (residues, 770-970) of KHC from either wild type or Ala-mutant, were subcloned into pET28(a+) kinesin light chain (a gift from Yao Wang in the lab of Dr. Sarah Rice at Northwestern University).

6.2 Cell culture

To select stable cell lines expressing EGFP-SKL (peroxisome-targeting signal) or Dendra2-tubulin with kinesin heavy chain (KHC) wild type or a KHC Ala-mutant, S2 cells were

cotransfected with three plasmids: (1) either pGG101 encoding EGFP-SKL (a gift from Dr. Gohta Goshima; UCSF) or pMT.A-Dendra2-tubulin, (2) either pMT.A-kinesin heavy chain (KHC) or pMT.A-kinesin A-mutant, and (3) pCoHygro (Invitrogen) as a selection plasmid, at a 5:20:1 molar ratio. To select stable cell lines expressing EGFP-SKL (peroxisome-targeting signal) and mRFP-p150^{glued} or mRFP-ΔN-p150^{glued}, S2 cells were cotransfected with three plasmids: pGG101 encoding EGFP-SKL, pCoHygro (Invitrogen) as a selection plasmid, and either pAc.A-mRFP-p150^{glued} or pAc.A-mRFP-ΔN-p150^{glued} at a 20:1:20 molar ratio. Transfection was performed using Cellfectin reagent (Invitrogen). Forty hours after transfection, Hygromycin (300 μg/ml) was added for selection. Selection was performed for 4-5 weeks and the protein expression was confirmed by fluorescence microscopy and immunoblotting.

Lysosomes in S2 cells were labeled by staining with 100 nM of LysoTracker Red DND-99 (Invitrogen) for 10 min. For endosome labeling, S2 cells in suspension were incubated with 1 mg/ml of Texas Red dextran (Invitrogen) for 6 hrs.

Expression of EGFP-EB1 was induced by addition of 30 μM of CuSO₄ overnight, and then cells were plated on ConA coverslips, and stimulated to grow processes by 5 μM of cytochalasin D. The temporal movements of EGFP-EB1 along processes were examined and recorded as vertical displacements using “kymograph” function in METAMORPH software. A total 204 EGFP-EB1-labeled microtubule tips in 52 thin processes (< 1 μm) were analyzed, which were 90 % toward outwards and 10 % toward cell body. A total of 100 EGFP-EB1-labeled microtubule tips in 31 thick (>1 μm or with lumps) processes were analyzed, which were 60 % toward outwards and 40 % toward cell body.

6.3. Double-stranded RNAi

RNAi treatment was performed as described by Ling et al (Ling et al., 2004b). Templates for *in vitro* transcription were generated by using the primers 5'-

TAATACGACTCACTATAGGGGTATCGTGGCAATGGAATCG-3' and 5'-

TAATACGACTCACTATAGGGGAGTTATAACAACATCAGCAA-3' to amplify the 500 bp from the 3' untranslated region of p150^{glued} and the primers 5'-

TAATACGACTCACTATAGGGACCACCTGCAAAGCGATATCG-3' and 5'-

TAATACGACTCACTATAGGGTTGCAGATACTCCGTCAGGAT-3' to amplify the 550 bp segment from the C terminus of the p150^{glued} gene.

Templates for *in vitro* transcription were generated by using the primers 5'-

TAATACGACTCACTATAGGGCAGAACGGTCACACTGGCGC-3' and 5'-

TAATACGACTCACTATAGGGTGCTTACAGGGCGGAGATAG-3' to amplify the 500 bp from the 5' untranslated region of kinesin heavy chain (KHC) and the primers 5'-

TAATACGACTCACTATAGGGGAGAACATCATCCTCACCAACG-3' and 5'-

TAATACGACTCACTATAGGGGTTCTTATCCTCGTGCACACT-3' to amplify the 500 bp segment from the N terminus of the KHC gene.

6.4 Antibodies

The recombinant His₆-tagged p150^{glued} fusion proteins containing residues 1-190 or 1073-1280 were expressed in *E. coli* and purified by Talon affinity chromatography. Rabbit immunization was done by Proteintech Group Inc (Chicago, IL). For Western analysis, 1:5,000 dilution of antiserum was used. An antibody against the DHC was from Dr. Jonathan Scholey

(University of California, Davis) and HD antibody against KHC was provided by Dr. Alexander Minin (Institute of Protein Research, Russian Academy of Sciences, Moscow, Russia). An antibody against p50 was a kind gift of Dr. Rahul Warrior (University of California, Irvine) (Duncan and Warrior, 2002) and Arp1 antibody was provided by Dr. Lawrence Goldstein (University of California, San Diego). SUK4 and 9E10.2 (anti-KHC and anti-myc antibody, respectively) were obtained from Developmental Studies Hybridoma Bank, Iowa City, IA.

6.5 Immunofluorescent Staining

Cells were incubated in extraction buffer containing 1% Triton X-100 in PBS for 2 min and fixed with 1% glutaraldehyde or cold methanol for 10 min. For microtubule or EGFP staining, this study used monoclonal antibody DM1- α against α -tubulin (1:2,000) and polyclonal affinity-purified EGFP antibody (1:200), respectively. For analysis of mitotic phenotype, cells were immunostained for both microtubules and mitosis-specific phosphorylated histone H3.

6.6 Immunoprecipitation

Approximately 1×10^8 cells were used for the immunoprecipitation assay. Cell pellets were resuspended at a ratio of 1:2 (w/v) in a homogenization buffer (50 mM Tris pH 7.5, 50 mM KCl, 0.1 mM EDTA, 2 mM MgCl_2 , 1 % NP-40, 5% glycerol, 1 mM DTT, 1 mM PMSF, 10 g/ml of each chymostatin, leupeptin, and pepstatin) and homogenized by using a 25-gauge syringe needle. Cell extracts were centrifuged at $15,000 \times g$ for 10 min and then at $200,000 \times g$ for 15 min. The resulting supernatants were incubated with antibodies (EGFP or preimmune rabbit IgG) prebound to Protein A-Sepharose (Amersham/GE Healthcare, Piscataway, NJ) for 2

hr at 4°C. The beads were washed and proteins were eluted into SDS sample buffer and analyzed by Western blotting.

6.7 Microscopy and Image Analysis

Images of live cells were acquired as described by Ling et al. (Ling et al., 2004b) using U2000 Perfect Focus microscope system (Nikon Instruments, Melville, NY). 100 W halogen bulb was used for fluorescence excitation to minimize photobleaching and phototoxicity.

Images were captured every 5 sec for 5 min for fluorescent microtubules. For photoconversion, cells were exposed with 405 nm wavelength of intense Mercury light for 5 or 10 sec. The movement of microtubules was analyzed by counting the number of microtubule segments moving across the photoactivated zone after 5 min. The average numbers were converted as percentage compared to the control (wild type) cells.

Images were captured every 1 sec for 2 min for EGFP-tagged peroxisomes, endosomes, and lysosomes and every 2 sec for 2 min for EGFP-tagged dFMRP. The movement of particles was analyzed by using automatic tracking software Diatrack (version 3.01) (Semasopht, North Epping, Australia). A threshold speed is 0.2 $\mu\text{m}/\text{sec}$ for peroxisomes, endosomes, and lysosomes, or 0.15 $\mu\text{m}/\text{sec}$ for dFMRP particles and movements slower than this threshold were excluded from the calculations. This study measured all runs longer than 2 μm for peroxisomes, 1.6 μm for endosomes and lysosomes, and 1 μm for dFMRP particles. The number of runs above the threshold was divided by the average number of particles in the analyzed areas of the image. This value was defined as the relative number of runs. At least three independent experiments

were analyzed for each condition, and five to six cells in each experiment were randomly chosen for recording and analysis.

For FIONA analysis, an Andor Model DV-860 BV was used. The equipment was a back-illuminated camera containing a 128 by 128 pixel sensor with 24 μm pixel size. A quarter of chip was used to achieve 1 msec per frame. The incidence beam angle was tuned to get the best signal to noise. The cells were maintained at 10°C. For details of measurement, see (Yildiz et al., 2003).

6.8. Sucrose density gradient centrifugation

Approximately 3×10^7 cells were pelleted and cell extract was prepared as described above. The clarified supernatant (about 500 μl) was layered on the top of 12 ml of 5-20 % linear sucrose density gradient prepared in the homogenization buffer without NP-40. After centrifugation at $150,000 \times g$ for 18 hr in a SW 40 rotor (Beckman), 0.5 ml fraction were collected, and analyzed by Western blotting using antibodies to EGFP, p150^{glued}, DHC, or KHC.

6.9 Microtubule pelleting assay

Microtubules were prepared by polymerization of bovine brain tubulin in the presence of 1 mM GTP and 20 μM Taxol at 37°C for 1 hr. The polymerized microtubules were mixed with recombinant proteins and layered on the top of 30 % glycerol cushion in BRB80 buffer (80 mM PIPES, pH 6.9, 1 mM EGTA, 1 mM MgCl_2) with 10 μM Taxol. Microtubules were pelleted by centrifugation at $150,000 \times g$ for 40 min in a SW 55 rotor (Beckman). The pellets were washed and resuspended in 30 μl of SDS-sample buffer.

REFERENCES

- Ahmad, F.J., Y. He, K.A. Myers, T.P. Hasaka, F. Francis, M.M. Black, and P.W. Baas. 2006. Effects of dynactin disruption and dynein depletion on axonal microtubules. *Traffic*. 7:524-37.
- Akhmanova, A., and C.C. Hoogenraad. 2005. Microtubule plus-end-tracking proteins: mechanisms and functions. *Curr Opin Cell Biol*. 17:47-54.
- Askham, J.M., K.T. Vaughan, H.V. Goodson, and E.E. Morrison. 2002. Evidence that an interaction between EB1 and p150(Glued) is required for the formation and maintenance of a radial microtubule array anchored at the centrosome. *Mol Biol Cell*. 13:3627-45.
- Baas, P.W., C. Vidya Nadar, and K.A. Myers. 2006. Axonal transport of microtubules: the long and short of it. *Traffic*. 7:490-8.
- Blangy, A., L. Arnaud, and E.A. Nigg. 1997. Phosphorylation by p34cdc2 protein kinase regulates binding of the kinesin-related motor HsEg5 to the dynactin subunit p150. *J Biol Chem*. 272:19418-24.
- Blasius, T.L., D. Cai, G.T. Jih, C.P. Toret, and K.J. Verhey. 2007. Two binding partners cooperate to activate the molecular motor Kinesin-1. *J Cell Biol*. 176:11-7.
- Boylan, K., M. Serr, and T. Hays. 2000. A molecular genetic analysis of the interaction between the cytoplasmic dynein intermediate chain and the glued (dynactin) complex. *Mol Biol Cell*. 11:3791-803.
- Bruno, K.S., J.H. Tinsley, P.F. Minke, and M. Plamann. 1996. Genetic interactions among cytoplasmic dynein, dynactin, and nuclear distribution mutants of *Neurospora crassa*. *Proc Natl Acad Sci U S A*. 93:4775-80.
- Brust-Mascher, I., G. Civelekoglu-Scholey, M. Kwon, A. Mogilner, and J.M. Scholey. 2004. Model for anaphase B: role of three mitotic motors in a switch from poleward flux to spindle elongation. *Proc Natl Acad Sci U S A*. 101:15938-43.
- Buffin, E., C. Lefebvre, J. Huang, M.E. Gagou, and R.E. Karess. 2005. Recruitment of Mad2 to the kinetochore requires the Rod/Zw10 complex. *Curr Biol*. 15:856-61.
- Burkhardt, J.K., C.J. Echeverri, T. Nilsson, and R.B. Vallee. 1997. Overexpression of the dynamitin (p50) subunit of the dynactin complex disrupts dynein-dependent maintenance of membrane organelle distribution. *J Cell Biol*. 139:469-84.

- Coy, D.L., W.O. Hancock, M. Wagenbach, and J. Howard. 1999. Kinesin's tail domain is an inhibitory regulator of the motor domain. *Nat Cell Biol.* 1:288-92.
- Culver-Hanlon, T.L., S.A. Lex, A.D. Stephens, N.J. Quintyne, and S.J. King. 2006. A microtubule-binding domain in dynactin increases dynein processivity by skating along microtubules. *Nat Cell Biol.*
- Deacon, S.W., A.S. Serpinskaya, P.S. Vaughan, M. Lopez Fanarraga, I. Vernos, K.T. Vaughan, and V.I. Gelfand. 2003. Dynactin is required for bidirectional organelle transport. *J Cell Biol.* 160:297-301.
- Echeverri, C.J., B.M. Paschal, K.T. Vaughan, and R.B. Vallee. 1996. Molecular characterization of the 50-kD subunit of dynactin reveals function for the complex in chromosome alignment and spindle organization during mitosis. *J Cell Biol.* 132:617-33.
- Fukuda, M., T.S. Kuroda, and K. Mikoshiba. 2002. Slac2-a/melanophilin, the missing link between Rab27 and myosin Va: implications of a tripartite protein complex for melanosome transport. *J Biol Chem.* 277:12432-6.
- Gennerich, A., A.P. Carter, S.L. Reck-Peterson, and R.D. Vale. 2007. Force-induced bidirectional stepping of cytoplasmic Dynein. *Cell.* 131:952-65.
- Goldstein, L.S., and S. Gunawardena. 2000. Flying through the drosophila cytoskeletal genome. *J Cell Biol.* 150:F63-8.
- Goshima, G., and R.D. Vale. 2003. The roles of microtubule-based motor proteins in mitosis: comprehensive RNAi analysis in the Drosophila S2 cell line. *J Cell Biol.* 162:1003-16.
- Gross, S.P. 2004. Hither and yon: a review of bi-directional microtubule-based transport. *Phys Biol.* 1:R1-11.
- Gross, S.P., M.A. Welte, S.M. Block, and E.F. Wieschaus. 2002. Coordination of opposite-polarity microtubule motors. *J Cell Biol.* 156:715-24.
- Gurskaya, N.G., V.V. Verkhusha, A.S. Shcheglov, D.B. Staroverov, T.V. Chepurnykh, A.F. Fradkov, S. Lukyanov, and K.A. Lukyanov. 2006. Engineering of a monomeric green-to-red photoactivatable fluorescent protein induced by blue light. *Nat Biotechnol.* 24:461-5.
- Hackney, D.D. 1995. Highly processive microtubule-stimulated ATP hydrolysis by dimeric kinesin head domains. *Nature.* 377:448-50.
- Hackney, D.D., and M.F. Stock. 2000. Kinesin's IAK tail domain inhibits initial microtubule-stimulated ADP release. *Nat Cell Biol.* 2:257-60.

- Hayashi, I., A. Wilde, T.K. Mal, and M. Ikura. 2005. Structural basis for the activation of microtubule assembly by the EB1 and p150Glued complex. *Mol Cell*. 19:449-60.
- He, Y., F. Francis, K.A. Myers, W. Yu, M.M. Black, and P.W. Baas. 2005. Role of cytoplasmic dynein in the axonal transport of microtubules and neurofilaments. *J Cell Biol*. 168:697-703.
- Holleran, E.A., S. Karki, and E.L. Holzbaur. 1998. The role of the dynactin complex in intracellular motility. *Int Rev Cytol*. 182:69-109.
- Holzbaur, E.L., and R.B. Vallee. 1994. DYNEINS: molecular structure and cellular function. *Annu Rev Cell Biol*. 10:339-72.
- Kamal, A., and L.S. Goldstein. 2002. Principles of cargo attachment to cytoplasmic motor proteins. *Curr Opin Cell Biol*. 14:63-8.
- Karcher, R.L., S.W. Deacon, and V.I. Gelfand. 2002. Motor-cargo interactions: the key to transport specificity. *Trends Cell Biol*. 12:21-7.
- Karki, S., and E.L. Holzbaur. 1995. Affinity chromatography demonstrates a direct binding between cytoplasmic dynein and the dynactin complex. *J Biol Chem*. 270:28806-11.
- Kerkhoff, E. 2006. Cellular functions of the Spir actin-nucleation factors. *Trends Cell Biol*. 16:477-83.
- Kim, H., S.C. Ling, G.C. Rogers, C. Kural, P.R. Selvin, S.L. Rogers, and V.I. Gelfand. 2007. Microtubule binding by dynactin is required for microtubule organization but not cargo transport. *J Cell Biol*. 176:641-51.
- King, S.J., C.L. Brown, K.C. Maier, N.J. Quintyne, and T.A. Schroer. 2003. Analysis of the dynein-dynactin interaction in vitro and in vivo. *Mol Biol Cell*. 14:5089-97.
- King, S.J., and T.A. Schroer. 2000. Dynactin increases the processivity of the cytoplasmic dynein motor. *Nat Cell Biol*. 2:20-4.
- Kobayashi, T., K. Shiroguchi, M. Edamatsu, and Y.Y. Toyoshima. 2006. Microtubule-binding properties of dynactin p150 expedient for dynein motility. *Biochem Biophys Res Commun*. 340:23-8.
- Kodama, A., I. Karakesisoglou, E. Wong, A. Vaezi, and E. Fuchs. 2003. ACF7: an essential integrator of microtubule dynamics. *Cell*. 115:343-54.
- Kural, C., H. Kim, S. Syed, G. Goshima, V.I. Gelfand, and P.R. Selvin. 2005. Kinesin and dynein move a peroxisome in vivo: a tug-of-war or coordinated movement? *Science*. 308:1469-72.

- Lai, C., X. Lin, J. Chandran, H. Shim, W.J. Yang, and H. Cai. 2007. The G59S mutation in p150(glued) causes dysfunction of dynactin in mice. *J Neurosci.* 27:13982-90.
- Lansbergen, G., Y. Komarova, M. Modesti, C. Wyman, C.C. Hoogenraad, H.V. Goodson, R.P. Lemaitre, D.N. Drechsel, E. van Munster, T.W. Gadella, Jr., F. Grosveld, N. Galjart, G.G. Borisy, and A. Akhmanova. 2004. Conformational changes in CLIP-170 regulate its binding to microtubules and dynactin localization. *J Cell Biol.* 166:1003-14.
- Levy, J.R., C.J. Sumner, J.P. Caviston, M.K. Tokito, S. Ranganathan, L.A. Ligon, K.E. Wallace, B.H. Lamonte, G.G. Harmison, I. Puls, K.H. Fischbeck, and E.L. Holzbaur. 2006. A motor neuron disease-associated mutation in p150Glued perturbs dynactin function and induces protein aggregation. *J Cell Biol.* 172:733-45.
- Ligon, L.A., S.S. Shelly, M. Tokito, and E.L. Holzbaur. 2003. The microtubule plus-end proteins EB1 and dynactin have differential effects on microtubule polymerization. *Mol Biol Cell.* 14:1405-17.
- Ligon, L.A., M. Tokito, J.M. Finklestein, F.E. Grossman, and E.L. Holzbaur. 2004. A direct interaction between cytoplasmic dynein and kinesin I may coordinate motor activity. *J Biol Chem.* 279:19201-8.
- Ling, S.C., P.S. Fahrner, W.T. Greenough, and V.I. Gelfand. 2004. Transport of Drosophila fragile X mental retardation protein-containing ribonucleoprotein granules by kinesin-1 and cytoplasmic dynein. *Proc Natl Acad Sci U S A.* 101:17428-33.
- Maddox, P., A. Desai, K. Oegema, T.J. Mitchison, and E.D. Salmon. 2002. Poleward microtubule flux is a major component of spindle dynamics and anaphase a in mitotic Drosophila embryos. *Curr Biol.* 12:1670-4.
- Maddox, P., A. Straight, P. Coughlin, T.J. Mitchison, and E.D. Salmon. 2003. Direct observation of microtubule dynamics at kinetochores in Xenopus extract spindles: implications for spindle mechanics. *J Cell Biol.* 162:377-82.
- Mallik, R., B.C. Carter, S.A. Lex, S.J. King, and S.P. Gross. 2004. Cytoplasmic dynein functions as a gear in response to load. *Nature.* 427:649-52.
- Mallik, R., and S.P. Gross. 2004. Molecular motors: strategies to get along. *Curr Biol.* 14:R971-82.
- Martin, M., S.J. Iyadurai, A. Gassman, J.G. Gindhart, Jr., T.S. Hays, and W.M. Saxton. 1999. Cytoplasmic dynein, the dynactin complex, and kinesin are interdependent and essential for fast axonal transport. *Mol Biol Cell.* 10:3717-28.
- Mehta, A.D., R.S. Rock, M. Rief, J.A. Spudich, M.S. Mooseker, and R.E. Cheney. 1999. Myosin-V is a processive actin-based motor. *Nature.* 400:590-3.

- Mimori-Kiyosue, Y., N. Shiina, and S. Tsukita. 2000. The dynamic behavior of the APC-binding protein EB1 on the distal ends of microtubules. *Curr Biol.* 10:865-8.
- Mimori-Kiyosue, Y., and S. Tsukita. 2003. "Search-and-capture" of microtubules through plus-end-binding proteins (+TIPs). *J Biochem (Tokyo).* 134:321-6.
- Miyamoto, D.T., Z.E. Perlman, K.S. Burbank, A.C. Groen, and T.J. Mitchison. 2004. The kinesin Eg5 drives poleward microtubule flux in *Xenopus laevis* egg extract spindles. *J Cell Biol.* 167:813-8.
- Morales-Mulia, S., and J.M. Scholey. 2005. Spindle pole organization in *Drosophila* S2 cells by dynein, abnormal spindle protein (Asp), and KLP10A. *Mol Biol Cell.* 16:3176-86.
- Myers, K.A., and P.W. Baas. 2007. Kinesin-5 regulates the growth of the axon by acting as a brake on its microtubule array. *In J Cell Biol.* Vol. 178. 1081-91.
- Navone, F., J. Niclas, N. Hom-Booher, L. Sparks, H.D. Bernstein, G. McCaffrey, and R.D. Vale. 1992. Cloning and expression of a human kinesin heavy chain gene: interaction of the COOH-terminal domain with cytoplasmic microtubules in transfected CV-1 cells. *J Cell Biol.* 117:1263-75.
- Nurminsky, D.I., M.V. Nurminskaya, E.V. Benevolenskaya, Y.Y. Shevelyov, D.L. Hartl, and V.A. Gvozdev. 1998. Cytoplasmic dynein intermediate-chain isoforms with different targeting properties created by tissue-specific alternative splicing. *Mol Cell Biol.* 18:6816-25.
- Oladipo, A., A. Cowan, and V. Rodionov. 2007. Microtubule motor Ncd induces sliding of microtubules in vivo. *Mol Biol Cell.* 18:3601-6.
- Park, H., E. Toprak, and P.R. Selvin. 2007. Single-molecule fluorescence to study molecular motors. *Q Rev Biophys.* 40:87-111.
- Puls, I., C. Jonnakuty, B.H. LaMonte, E.L. Holzbaur, M. Tokito, E. Mann, M.K. Floeter, K. Bidus, D. Drayna, S.J. Oh, R.H. Brown, Jr., C.L. Ludlow, and K.H. Fischbeck. 2003. Mutant dynactin in motor neuron disease. *Nat Genet.* 33:455-6.
- Quintyne, N.J., S.R. Gill, D.M. Eckley, C.L. Crego, D.A. Compton, and T.A. Schroer. 1999. Dynactin is required for microtubule anchoring at centrosomes. *J Cell Biol.* 147:321-34.
- Quintyne, N.J., J.E. Reing, D.R. Hoffelder, S.M. Gollin, and W.S. Saunders. 2005. Spindle multipolarity is prevented by centrosomal clustering. *Science.* 307:127-9.
- Quintyne, N.J., and T.A. Schroer. 2002. Distinct cell cycle-dependent roles for dynactin and dynein at centrosomes. *J Cell Biol.* 159:245-54.

- Reck-Peterson, S.L., A. Yildiz, A.P. Carter, A. Gennerich, N. Zhang, and R.D. Vale. 2006. Single-molecule analysis of dynein processivity and stepping behavior. *Cell*. 126:335-48.
- Reilein, A., and W.J. Nelson. 2005. APC is a component of an organizing template for cortical microtubule networks. *Nat Cell Biol*. 7:463-73.
- Robinson, J.T., E.J. Wojcik, M.A. Sanders, M. McGrail, and T.S. Hays. 1999. Cytoplasmic dynein is required for the nuclear attachment and migration of centrosomes during mitosis in *Drosophila*. *J Cell Biol*. 146:597-608.
- Rodionov, V.I., and G.G. Borisy. 1997. Microtubule treadmilling in vivo. *Science*. 275:215-8.
- Rogers, G.C., S.L. Rogers, T.A. Schwimmer, S.C. Ems-McClung, C.E. Walczak, R.D. Vale, J.M. Scholey, and D.J. Sharp. 2004. Two mitotic kinesins cooperate to drive sister chromatid separation during anaphase. *Nature*. 427:364-70.
- Rogers, S.L., G.C. Rogers, D.J. Sharp, and R.D. Vale. 2002. *Drosophila* EB1 is important for proper assembly, dynamics, and positioning of the mitotic spindle. *J Cell Biol*. 158:873-84.
- Rosales-Nieves, A.E., J.E. Johndrow, L.C. Keller, C.R. Magie, D.M. Pinto-Santini, and S.M. Parkhurst. 2006. Coordination of microtubule and microfilament dynamics by *Drosophila* Rho1, Spire and Cappuccino. *Nat Cell Biol*. 8:367-76.
- Schliwa, M., and G. Woehlke. 2003. Molecular motors. *Nature*. 422:759-65.
- Schroer, T.A. 2004. Dynactin. *Annu Rev Cell Dev Biol*. 20:759-79.
- Schroer, T.A., and M.P. Sheetz. 1991. Two activators of microtubule-based vesicle transport. *J Cell Biol*. 115:1309-18.
- Serbus, L.R., B.J. Cha, W.E. Theurkauf, and W.M. Saxton. 2005. Dynein and the actin cytoskeleton control kinesin-driven cytoplasmic streaming in *Drosophila* oocytes. *Development*. 132:3743-52.
- Sharp, D.J., H.M. Brown, M. Kwon, G.C. Rogers, G. Holland, and J.M. Scholey. 2000a. Functional coordination of three mitotic motors in *Drosophila* embryos. *Mol Biol Cell*. 11:241-53.
- Sharp, D.J., G.C. Rogers, and J.M. Scholey. 2000b. Cytoplasmic dynein is required for poleward chromosome movement during mitosis in *Drosophila* embryos. *Nat Cell Biol*. 2:922-30.
- Soldati, T., and M. Schliwa. 2006. Powering membrane traffic in endocytosis and recycling. *Nat Rev Mol Cell Biol*. 7:897-908.

- Straube, A., G. Hause, G. Fink, and G. Steinberg. 2006. Conventional kinesin mediates microtubule-microtubule interactions in vivo. *Mol Biol Cell*. 17:907-16.
- Svoboda, K., C.F. Schmidt, B.J. Schnapp, and S.M. Block. 1993. Direct observation of kinesin stepping by optical trapping interferometry. *Nature*. 365:721-7.
- Thorn, K.S., J.A. Ubersax, and R.D. Vale. 2000. Engineering the processive run length of the kinesin motor. *J Cell Biol*. 151:1093-100.
- Tokito, M.K., D.S. Howland, V.M. Lee, and E.L. Holzbaur. 1996. Functionally distinct isoforms of dynactin are expressed in human neurons. *Mol Biol Cell*. 7:1167-80.
- Vale, R.D., and R.A. Milligan. 2000. The way things move: looking under the hood of molecular motor proteins. *Science*. 288:88-95.
- Vallee, R.B., J.C. Williams, D. Varma, and L.E. Barnhart. 2004. Dynein: An ancient motor protein involved in multiple modes of transport. *J Neurobiol*. 58:189-200.
- Vaughan, K.T. 2005a. Microtubule plus ends, motors, and traffic of Golgi membranes. *Biochim Biophys Acta*. 1744:316-24.
- Vaughan, K.T. 2005b. TIP maker and TIP marker; EB1 as a master controller of microtubule plus ends. *J Cell Biol*. 171:197-200.
- Vaughan, K.T., S.H. Tynan, N.E. Faulkner, C.J. Echeverri, and R.B. Vallee. 1999. Colocalization of cytoplasmic dynein with dynactin and CLIP-170 at microtubule distal ends. *J Cell Sci*. 112 (Pt 10):1437-47.
- Vaughan, K.T., and R.B. Vallee. 1995. Cytoplasmic dynein binds dynactin through a direct interaction between the intermediate chains and p150Glued. *J Cell Biol*. 131:1507-16.
- Vaughan, P.S., P. Miura, M. Henderson, B. Byrne, and K.T. Vaughan. 2002. A role for regulated binding of p150(Glued) to microtubule plus ends in organelle transport. *J Cell Biol*. 158:305-19.
- Verhey, K.J., D.L. Lizotte, T. Abramson, L. Barenboim, B.J. Schnapp, and T.A. Rapoport. 1998. Light chain-dependent regulation of Kinesin's interaction with microtubules. *J Cell Biol*. 143:1053-66.
- Verhey, K.J., D. Meyer, R. Deehan, J. Blenis, B.J. Schnapp, T.A. Rapoport, and B. Margolis. 2001. Cargo of kinesin identified as JIP scaffolding proteins and associated signaling molecules. *J Cell Biol*. 152:959-70.

- Waterman-Storer, C.M., S. Karki, and E.L. Holzbaur. 1995. The p150Glued component of the dynactin complex binds to both microtubules and the actin-related protein centractin (Arp-1). *Proc Natl Acad Sci U S A*. 92:1634-8.
- Waterman-Storer, C.M., S.B. Karki, S.A. Kuznetsov, J.S. Tabb, D.G. Weiss, G.M. Langford, and E.L. Holzbaur. 1997. The interaction between cytoplasmic dynein and dynactin is required for fast axonal transport. *Proc Natl Acad Sci U S A*. 94:12180-5.
- Watson, P., and D.J. Stephens. 2006. Microtubule plus-end loading of p150(Glued) is mediated by EB1 and CLIP-170 but is not required for intracellular membrane traffic in mammalian cells. *J Cell Sci*. 119:2758-67.
- Wojcik, E., R. Basto, M. Serr, F. Scaerou, R. Karess, and T. Hays. 2001. Kinetochore dynein: its dynamics and role in the transport of the Rough deal checkpoint protein. *Nat Cell Biol*. 3:1001-7.
- Wu, X.S., K. Rao, H. Zhang, F. Wang, J.R. Sellers, L.E. Matesic, N.G. Copeland, N.A. Jenkins, and J.A. Hammer, 3rd. 2002. Identification of an organelle receptor for myosin-Va. *Nat Cell Biol*. 4:271-8.
- Yildiz, A., J.N. Forkey, S.A. McKinney, T. Ha, Y.E. Goldman, and P.R. Selvin. 2003. Myosin V walks hand-over-hand: single fluorophore imaging with 1.5-nm localization. *Science*. 300:2061-5.
- Yildiz, A., M. Tomishige, R.D. Vale, and P.R. Selvin. 2004a. Kinesin walks hand-over-hand. *Science*. 303:676-8.
- Yildiz, A., M. Tomishige, R.D. Vale, and P.R. Selvin. 2004b. Kinesin Walks Hand-Over-Hand. *Science*. 303:676-678.

CURRICULUM VITAE

Hwajin Kim

*Northwestern Feinberg Medical School
303 E. Chicago, Ward 11-100
Chicago, IL 60611
hwajin-kim@northwestern.edu*

Education**Ph.D., Northwestern University, Chicago, IL**

Cell and Molecular Biology, June 2008

M.S., University of Illinois, Urbana-Champaign, IL

Molecular and Integrative Physiology, 2001

B.S., Sogang University, Seoul, Korea

Biology (Minor in Education), 1994-1998

Experiences**Doctoral research**

- Research project: The role of dynactin in microtubule-dependent organelle transport and coordination between opposite polarity motor proteins
- Studied how multiple motors work together in a coordinated manner
- Determined that microtubule binding by dynactin is required for spindle assembly, but not for organelle transport
- Determined that conventional kinesin is required for transporting microtubules
- Developed a *Drosophila* culture cell system for microtubule-based transport studies

Masters research

- Research project: The transcriptional regulation of *CYP450* genes and cross-talk between nuclear receptors involved in drug and lipid metabolism
- Demonstrated that nuclear receptor activated by xenobiotics regulates estrogen receptor function in reproductive physiology
- Determined the role of a mSin3A-Swi/Snf chromatin remodeling complex in feedback repression of bile acid synthesis
- Developed protocol for *in vivo* chromatin immunoprecipitation

Teaching Assistant

University of Illinois, Urbana-Champaign, IL (2003)

- Led undergraduate laboratory class of 20 students in Human Physiology
- Organized lectures and experimental materials and graded students based on quizzes

Publications

Kim H, Ling S, Rogers GC, Kural C, Selvin PR, Rogers SL, Gelfand VI. Microtubule binding by dynactin is required for microtubule organization but not cargo transport.

J. Cell Biol. 2007 176: 641-651. (Published Feb 26 2007 with its cover image)

Kural C, **Kim H**, Syed S, Goshima G, Gelfand VI, Selvin PR.

Kinesin and dynein move a peroxisome in vivo: a tug-of-war or coordinated movement?

Science 2005 Jun; 308(5727):1469-72.

Kemper JK*, **Kim H***, Miao J, Bhalla S, Bae Y.

Role of an mSin3A-Swi/Snf chromatin remodeling complex in the feedback repression of bile acid biosynthesis by SHP. **Mol Cell Biol. 2004 Sep; 24(17):7707-19.**

Petz LN, Ziegler YS, Schultz JR, **Kim H**, Kemper JK, Nardulli AM.

Differential regulation of the human progesterone receptor gene through an estrogen response element half site and Sp1 sites.

J Steroid Biochem Mol Biol. 2004 Feb; 88(2):113-22.

Goodwin B, Watson MA, **Kim H**, Miao J, Kemper JK, Kliewer SA.

Differential regulation of rat and human CYP7A1 by the nuclear oxysterol receptor liver X receptor- α . **Mol Endocrinol. 2003 Mar; 17(3):386-94.**

Min G*, **Kim H***, Bae Y, Petz L, Kemper JK.

Inhibitory cross-talk between estrogen receptor (ER) and constitutively activated androstane receptor (CAR). CAR inhibits ER-mediated signaling pathway by squelching p160 coactivators. **J Biol Chem. 2002 Sep; 277(37):34626-33.**

* Two authors contributed equally to this study.

Selected Presentations

- **47th American Society of Cell Biology meeting, Washington, DC**
“Microtubule Movement *in vivo* by Conventional Kinesin” (poster presentation, Dec, 2007)
- **Gordon Research Conference on Motile & Contractile Systems, New London, NH**
“Microtubule Movement *in vivo* by Conventional Kinesin” (poster presentation, July, 2007)
- **46th American Society of Cell Biology meeting, San Diego, CA**
“Microtubule binding by dynactin is required for microtubule organization but not cargo transport” (poster presentation, Dec., 2006)
- **Chicago Cytoskeleton, Northwestern Feinberg Medical School, Chicago, IL**
“The role of dynactin in microtubule-dependent organelle transport”
(Oral presentation, Nov., 2006)
- **Keystone Symposia, “Nuclear Receptor Superfamily”, Snowbird, Utah**
“Molecular mechanism of the bile acid-mediated transcriptional repression of the human cholesterol 7- α hydroxylase (CYP7A1)” (poster presentation, 2002)

Awards

- Predoctoral Student Travel Award, American Society of Cell Biology (Dec., 2006)
- Katten Muchin Rosenman Travel Scholarship Award, the Robert H. Lurie Comprehensive Cancer Center of Northwestern University (July, 2007)